Lecture 9. Stellar evolution in binary systems. Roche model. Evolutionary scenarios for massive and low-mass binaries. Non-conservative evolution (common envelopes, gravitational radiation, magnetic stellar wind)

Roche Model

- **Stars deform in close binary systems**
  - tides
  - rotation
- **Observations**
  - light curve effects from aspherical distortions
- **Small perturbations -- Legendre Polynomials**
- **Large deformations-- Roche Model**

Roche Potential

Assumes:

- **synchronous rotation**
- **circular orbit**
- **2 point masses**
- **rotating frame**

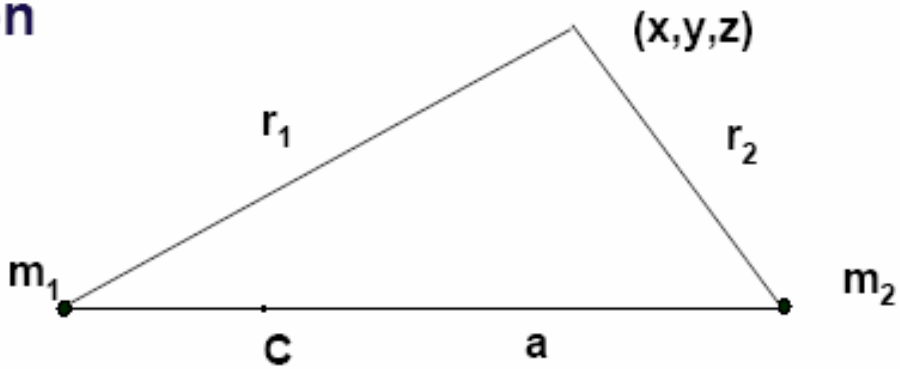

$$\omega^2 = \left(\frac{2\pi}{P}\right)^2 = \frac{G\,M}{a^3}$$

$$r_1^{\,2} = x^2 + y^2 + z^2 \qquad r_2^{\,2} = (x-a)^2 + y^2 + z^2$$

$$\frac{x_c}{a} = \frac{m_2}{M} = \frac{q}{1+q} \qquad q \equiv \frac{m_2}{m_1} \le 1$$

$$\Phi = -\frac{G\,m_1}{r_1} - \frac{G\,m_2}{r_2} - \frac{\omega^2}{2}\left[(x-x_c)^2 + y^2\right]$$

Dimensionless Roche Potential

factor out $-\frac{\omega^2}{2} = -\frac{G\,M}{2\,a^3}$ and $x \to \frac{x}{a}$, etc.

$$\Phi(x,y,z) = -\frac{\omega^2}{2}\,\Phi_N\left(\frac{x}{a},\frac{y}{a},\frac{z}{a},\right)$$

dimensionless Roche Potential:

$$\Phi_N(x,y,z) = \frac{2}{(1+q)}\frac{1}{r_1} + \frac{2\,q}{(1+q)}\frac{1}{r_2} + \left(x - \frac{q}{(1+q)}\right)^2 + y^2$$

Describes shape of potential surfaces independently of the mass and size of the system.

single parameter : q

Slice along X axis

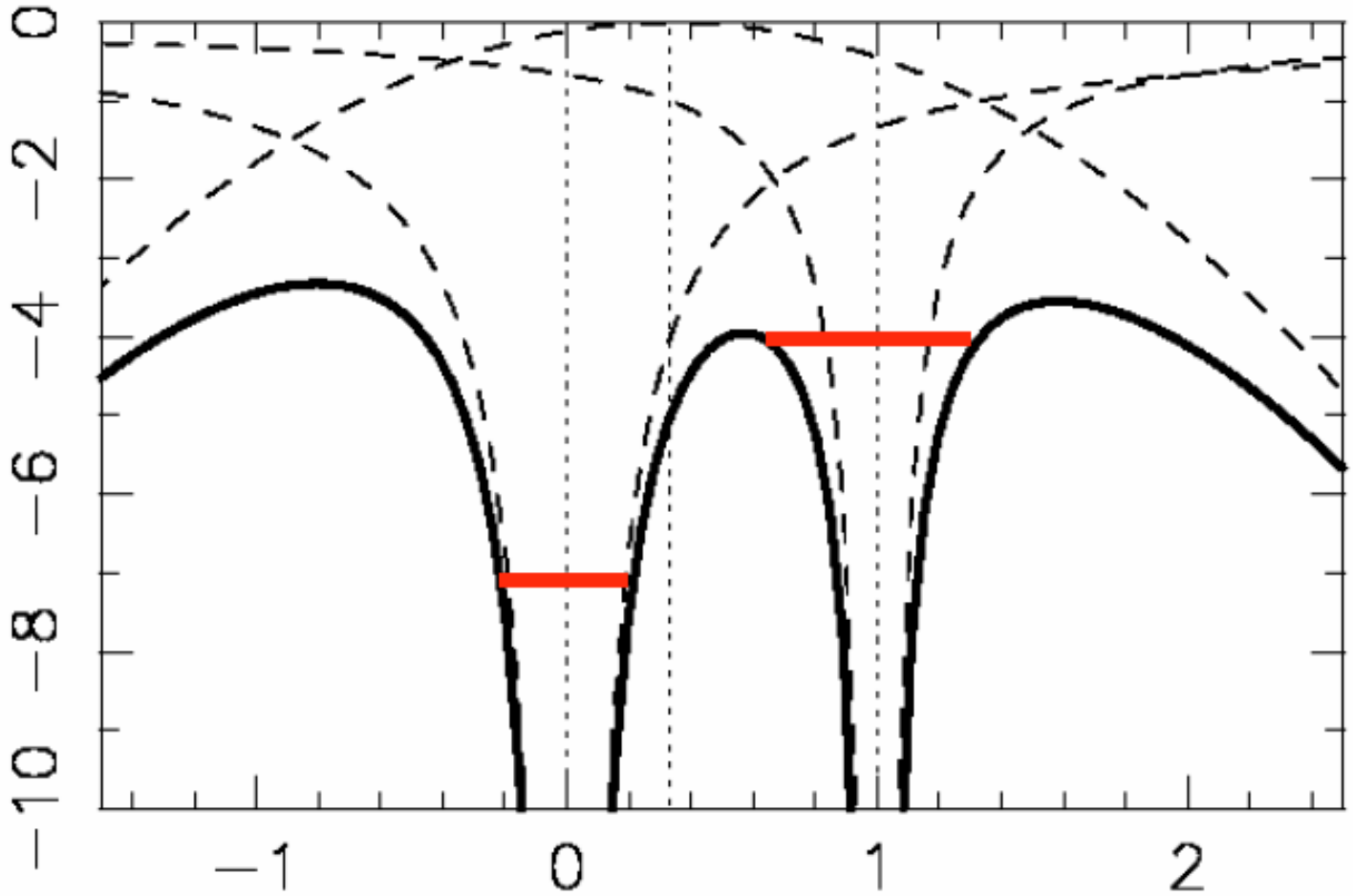

Potential in X-Y plane

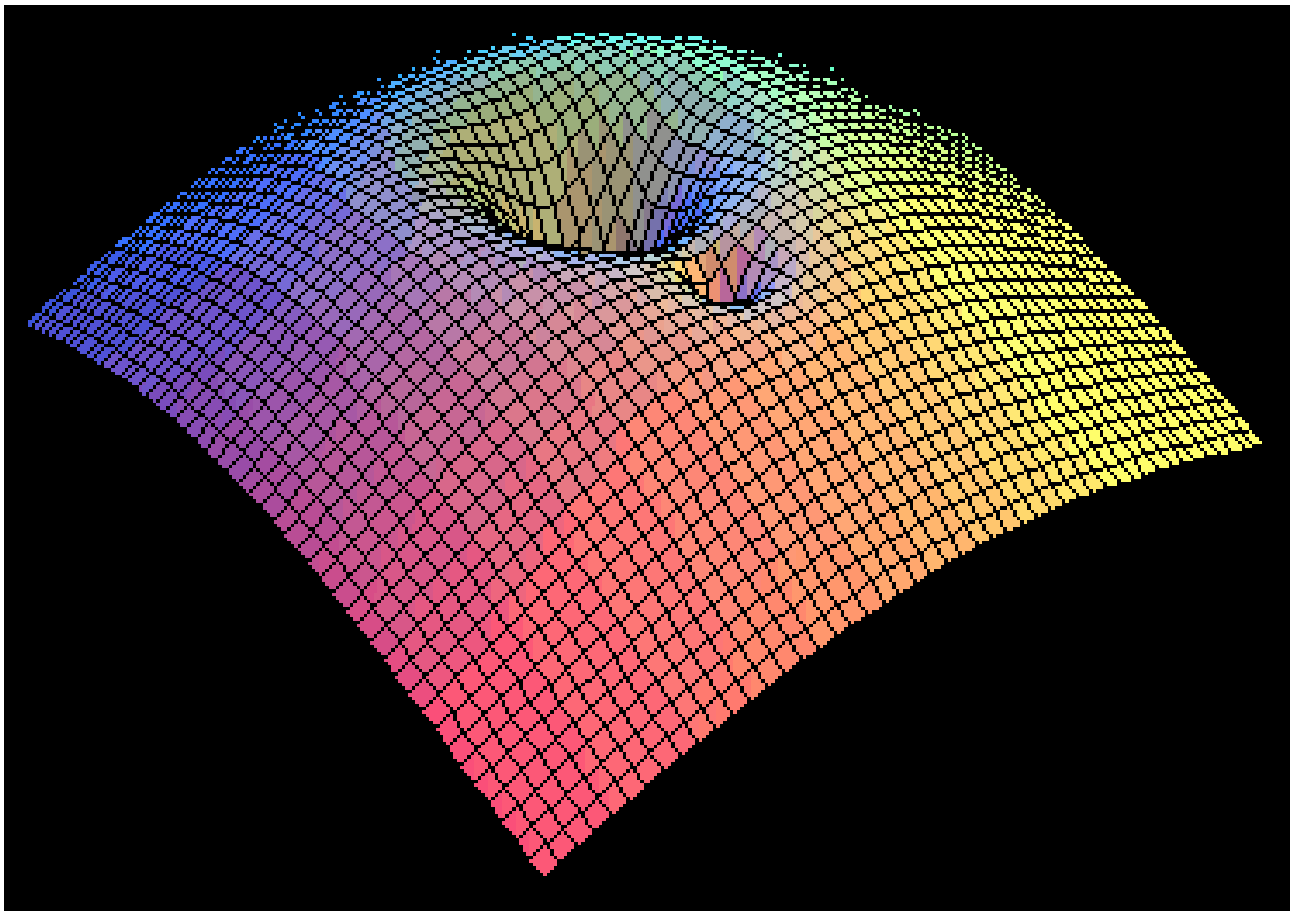

Roche Lobes

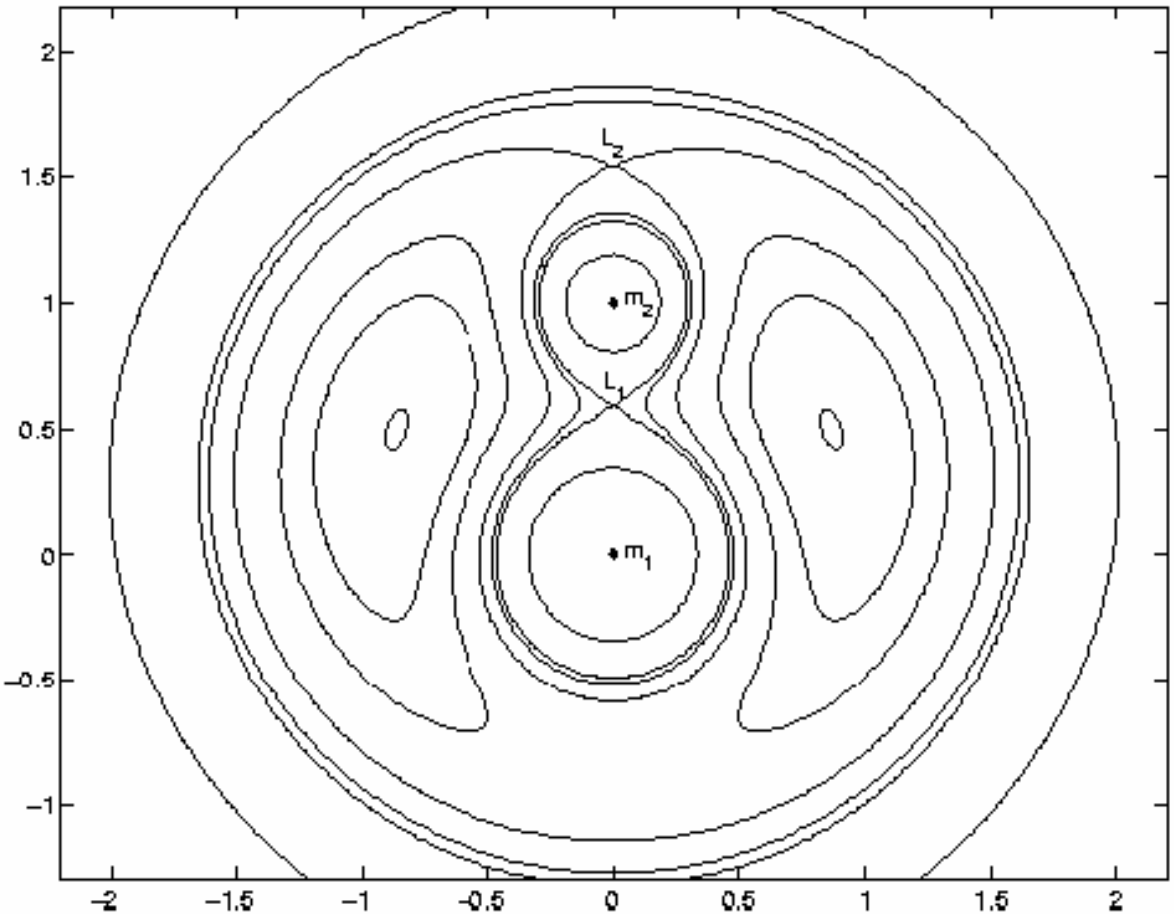

- Lagrange points L_1, L_2, L_3, and L_4, L_5

Lagrange points

- **Points where** $\nabla \Phi_n = 0$
- **L_1 - *Inner Lagrange Point***
  - in between two stars
  - matter can flow freely from one star to other
  - mass exhange
- **L_2 - on opposite side of secondary**
  - matter can most easily leave system
- **L_3 - on opposite side of primary**
- **L_4, L_5 - in lobes perpendicular to line joining binary**
  - form equilateral triangles with centres of two stars
- **Roche-lobes:: surfaces which just touch at L_1**
  - maximum size of non-contact systems

Roche Lobe Volumes

- **Effective size**
  - radius of Roche-lobe R_L
  - fit to results of numerical integration
  - Eggleton formula:

$$\frac{R_L}{a} \approx \frac{0.49 q^{2/3}}{0.69 q^{2/3} + \ln\left(1 + q^{1/3}\right)} a$$

- **Effectively, it is a tidal radius where**
  - mean density in lobes are equal

$$\frac{R_{L,2}}{a} \approx \frac{1}{2}\left(\frac{m_2}{M}\right)^{1/3} \quad \text{for } 0 \le q \le 0.8$$

Roche Lobes

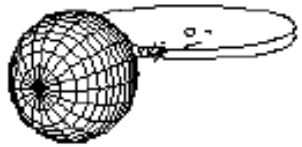

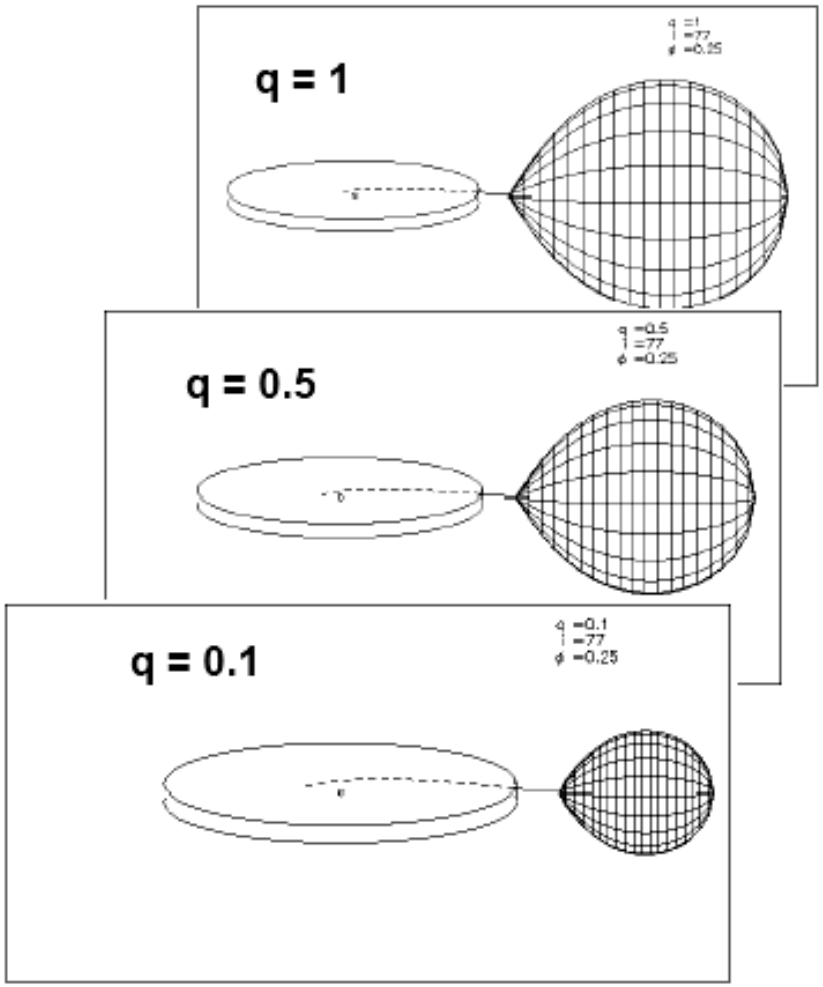

eclipses

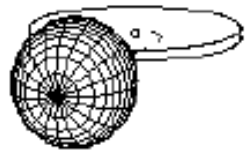

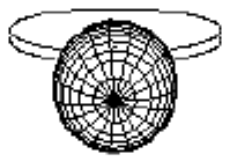

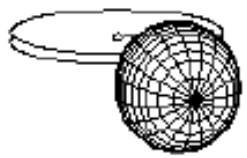

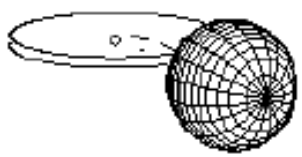

Proximity Effects

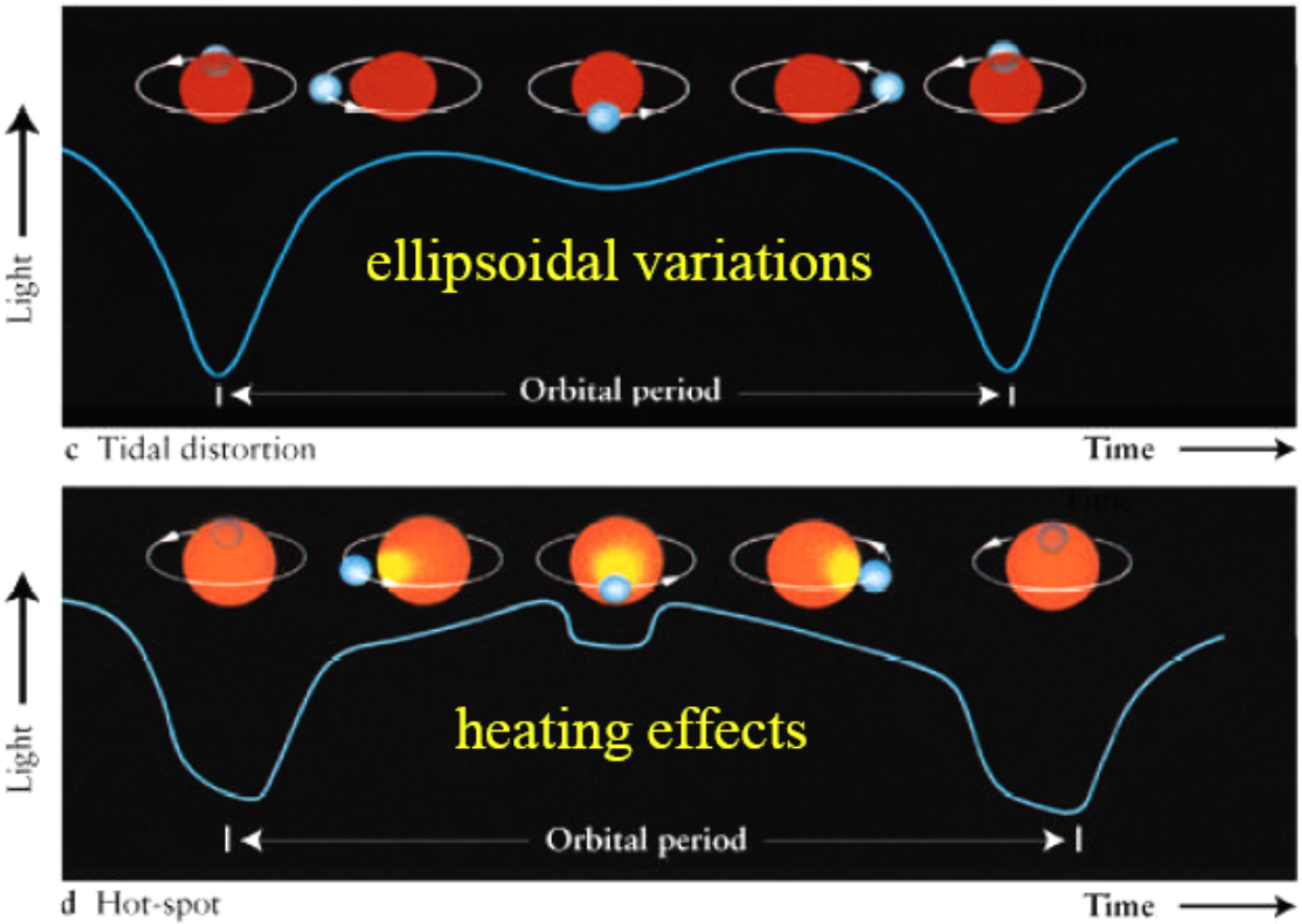

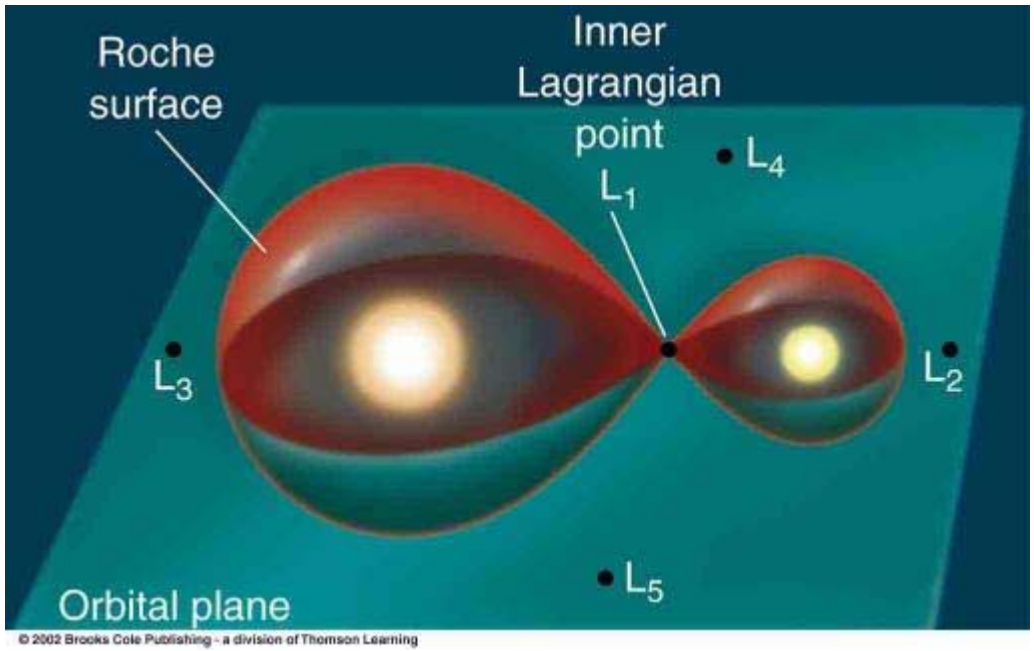
Roche
surface
Inner
Lagrangian
point
L_1
L_4
L_3
L_2
L_5
Orbital plane
© 2002 Brooks Cole Publishing - a division of Thomson Learning

Binaries in Roche-Lobes

detached

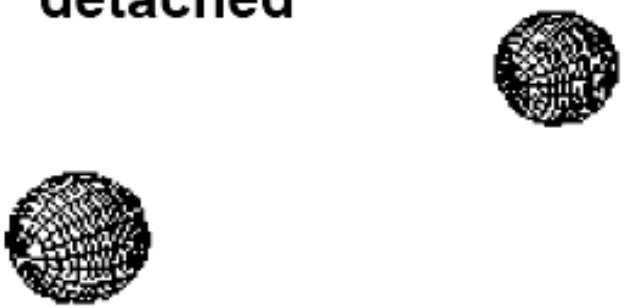

semi-detached
(Algol)

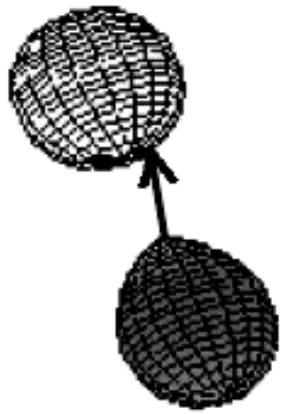

close to contact

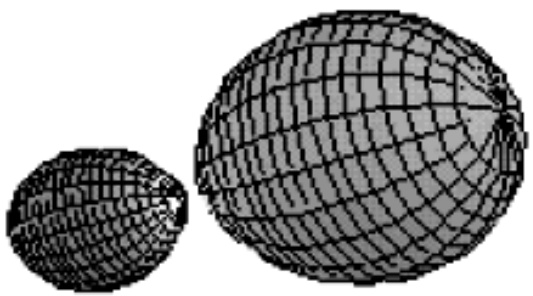

contact (W UMa)

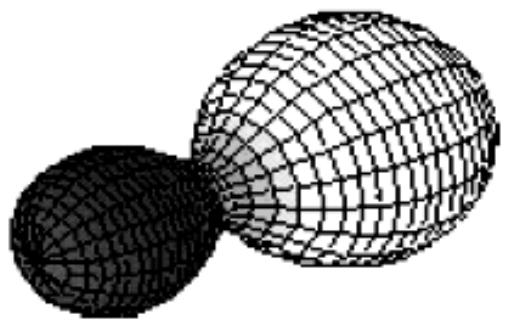

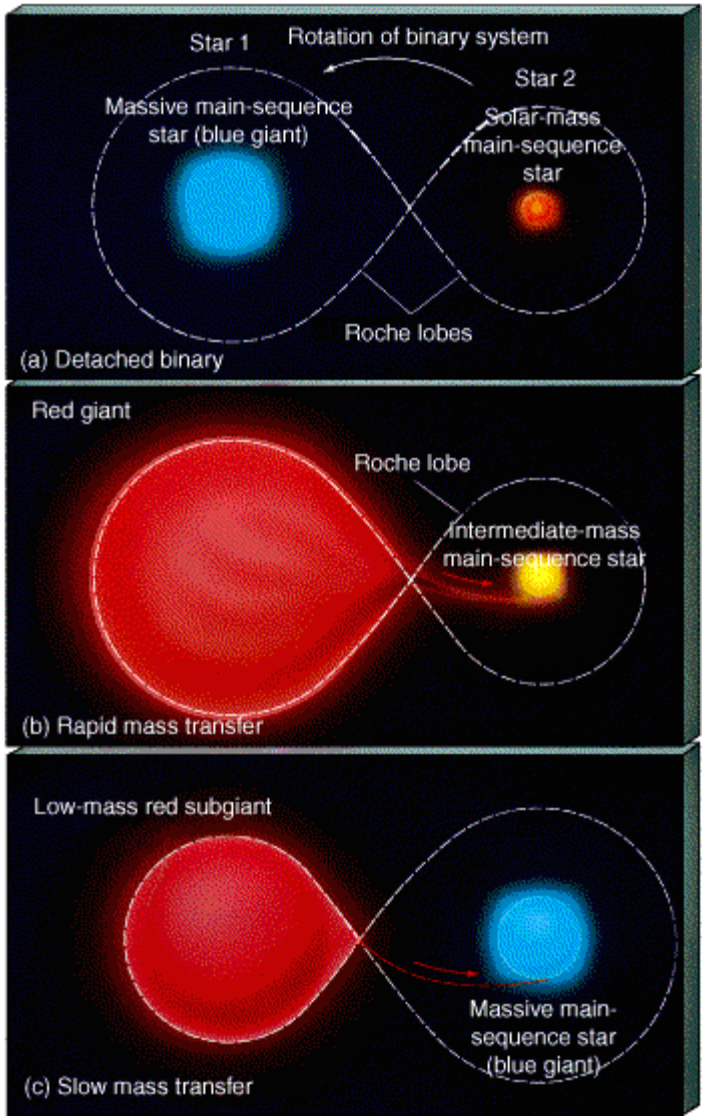

Algol (β Per) paradox: early-type component is heavier than the late-type one!

Key to solution: component mass reversal due to mass transfer at earlier stages!

0.8 $M_\odot$ G5IV 3.7 B8 V

Mass transfer and loss

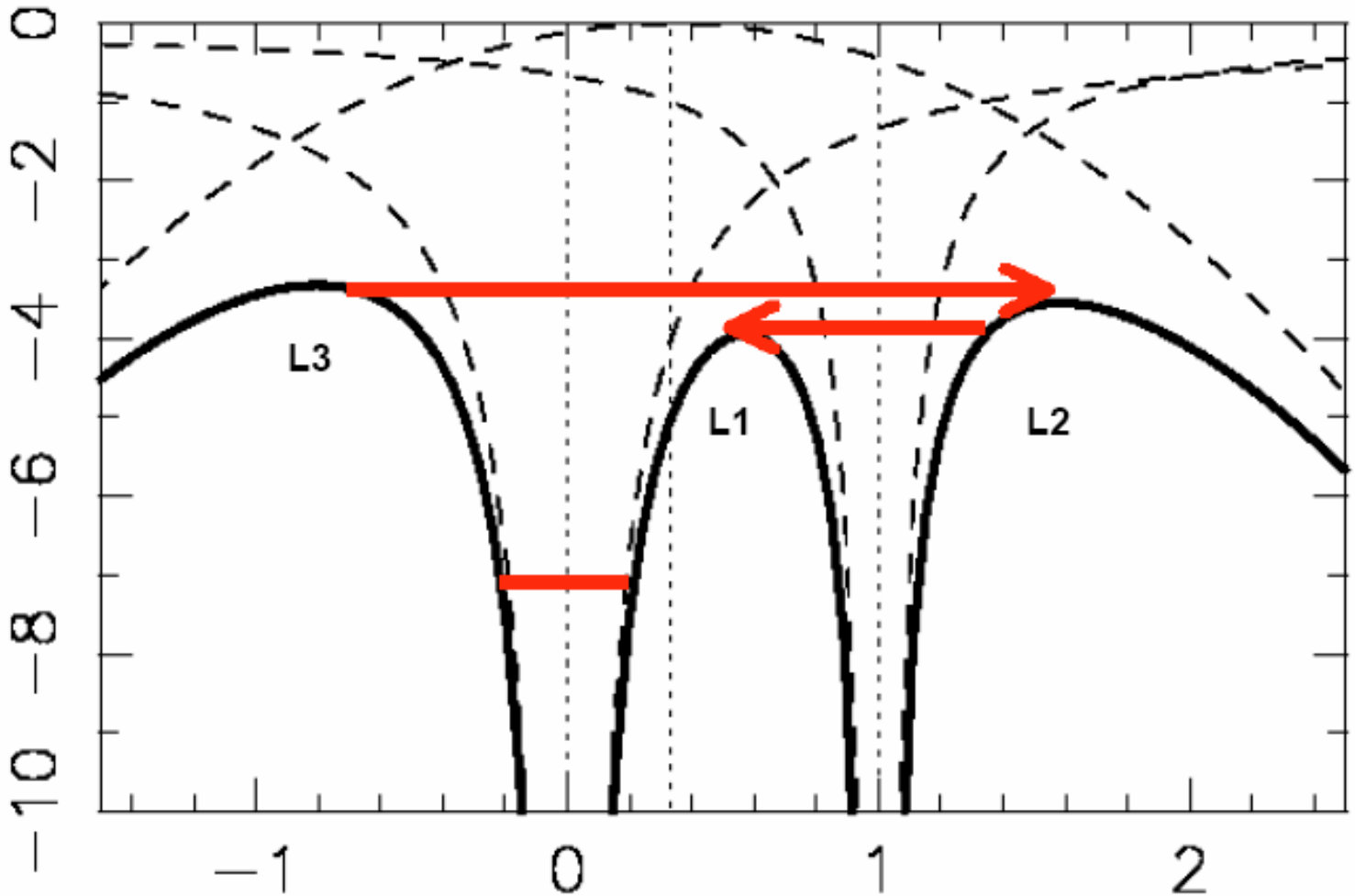

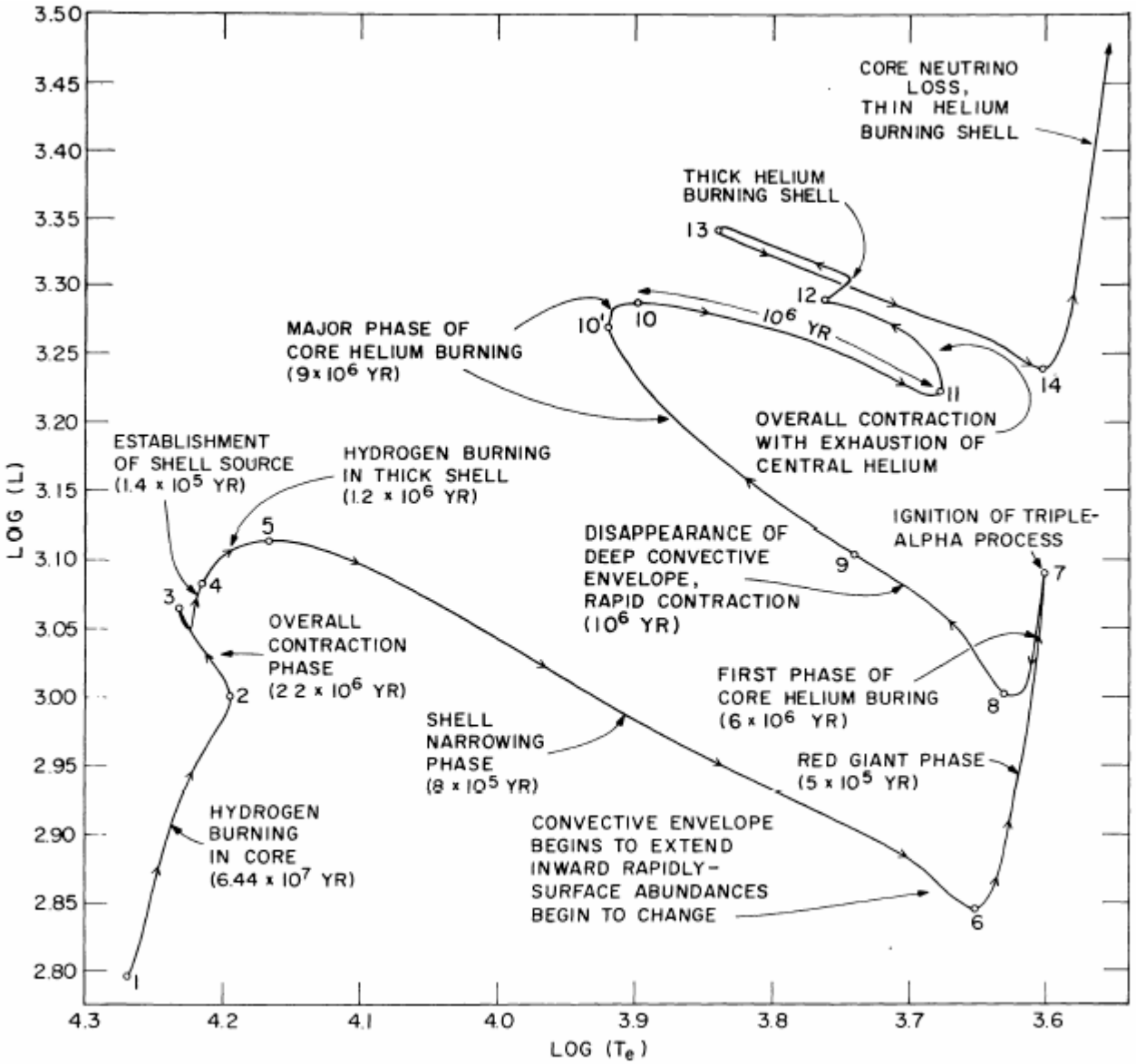

FIG. 2.—The track in the H-R diagram of a theoretical model star of mass 5 $M_\odot$ and of Population I composition. Text beside various portions of the track describe an important physical process occurring within the star at the indicated position. From Iben (1967*c*).

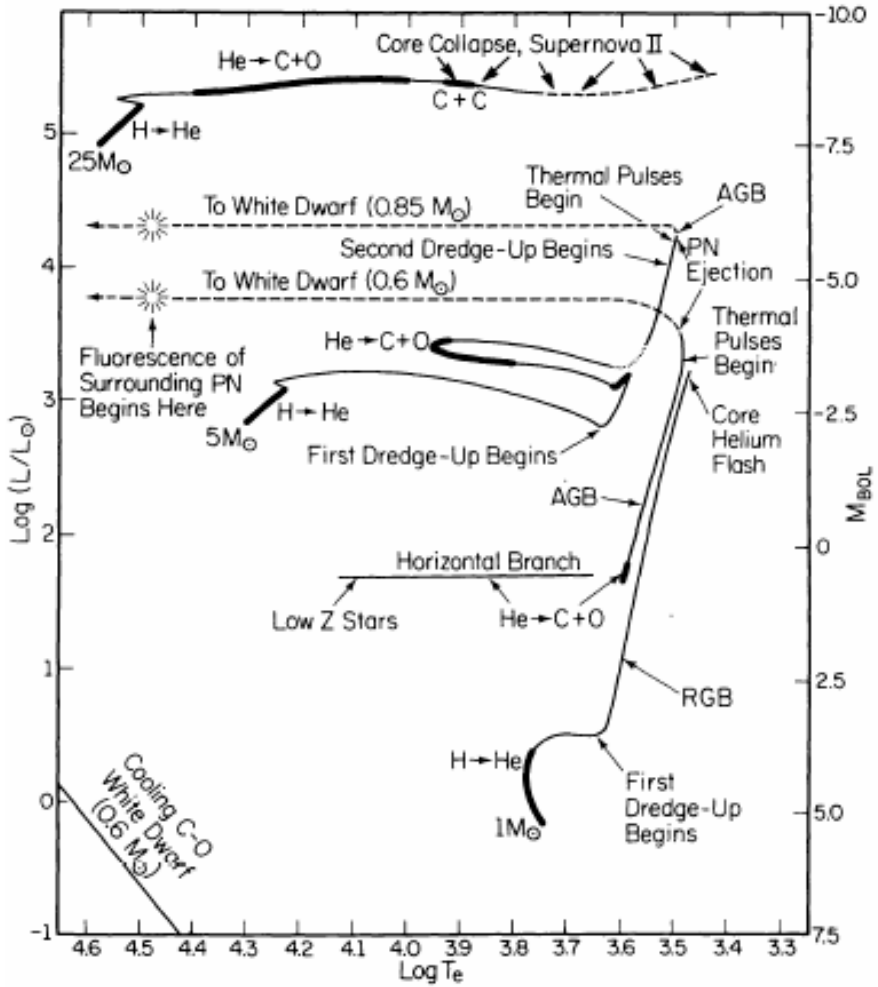

FIG. 5.—Tracks in the H-R diagram of theoretical model stars of low (1 $M_\odot$), intermediate (5 $M_\odot$), and high (25 $M_\odot$) mass. Nuclear burning on a long time scale occurs along the heavy portions of each track. The places

Mass loss depends on which stage of evolution the star fills its Roche lobe

If star is isentropic (e.g. deep convective envelope -- RG stage), mass loss tends to increase R with decreasing M which generally leads to unstable mass transfer

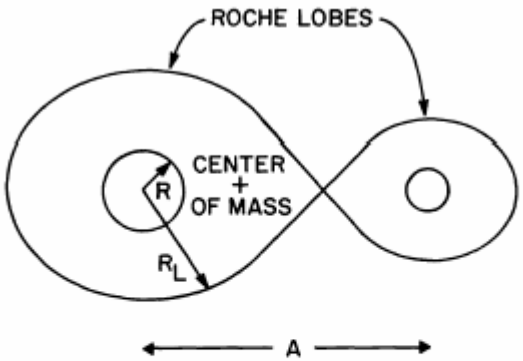

$$R_{iL} \sim 0.52 \left(\frac{m_i}{m_{tot}}\right)^{0.44} A$$

WHEN $R_i > R_{iL}$

$\Longrightarrow$ ROCHE-LOBE OVERFLOW

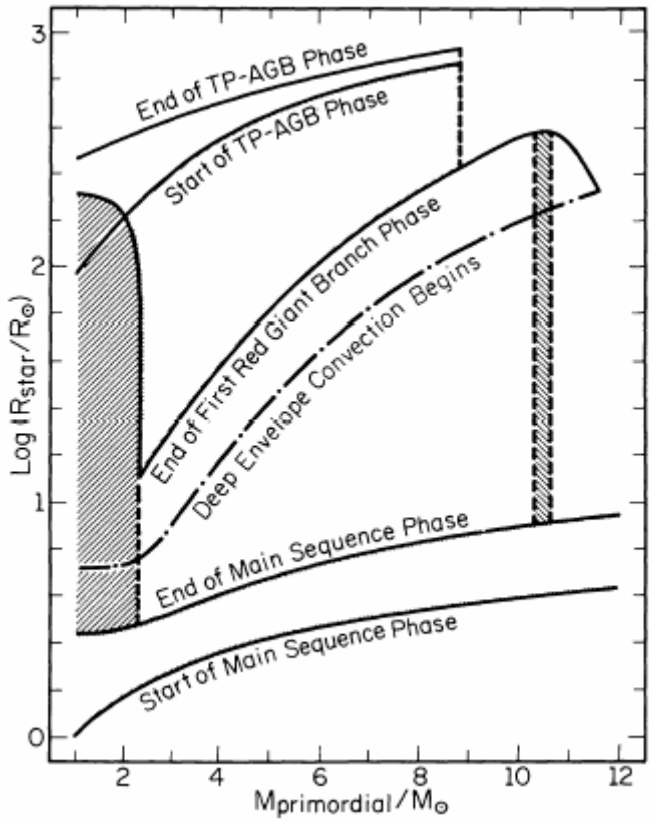

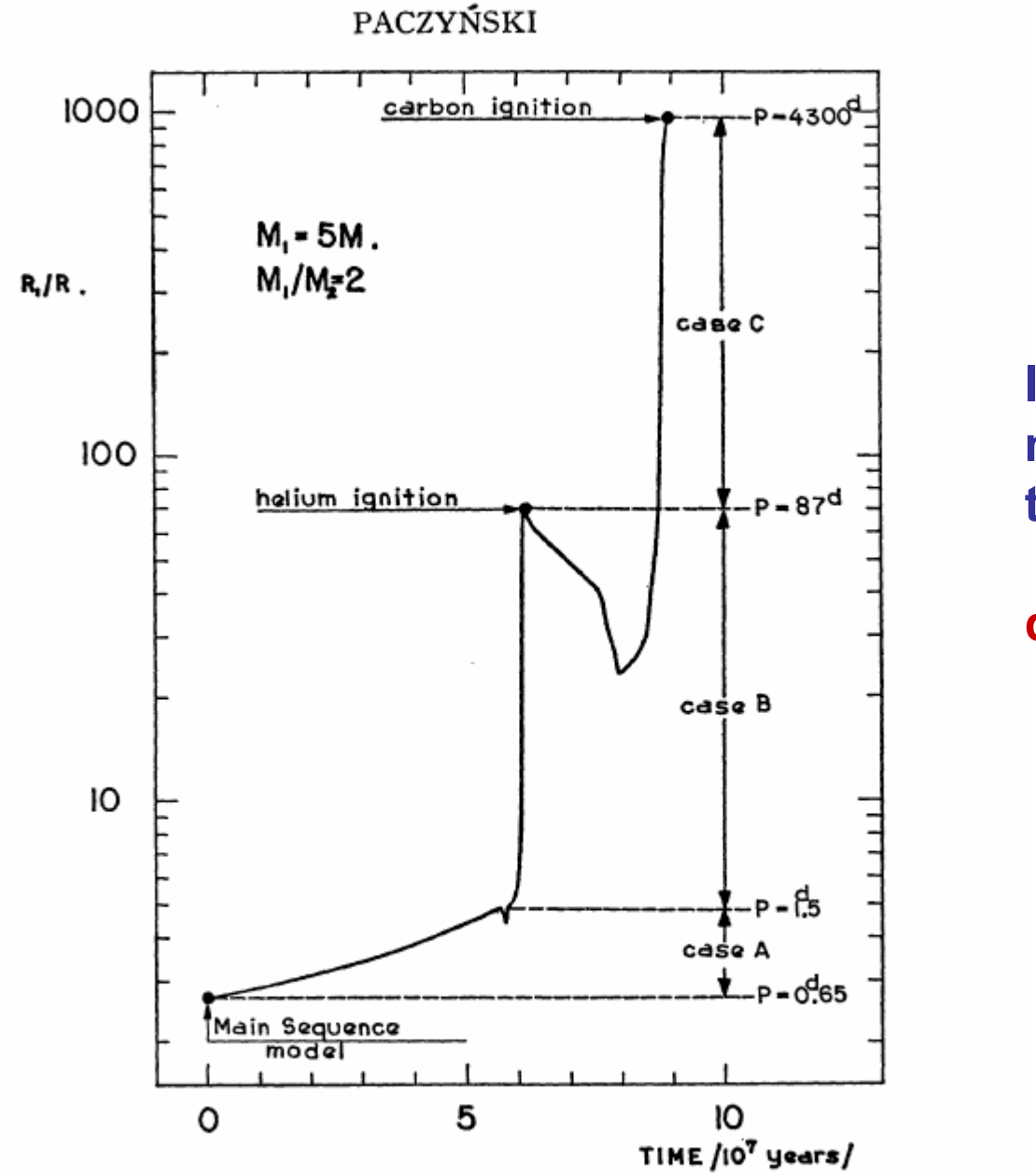

URE 1. The time variation of the radius of a 5 $M_\odot$ star. The ranges of orbital corresponding to the evolution with mass exchange in cases A, B, and C are d. A mass ratio of $M_1/M_2=2$ is adopted.

Three cases of mass transfer loss by the primary star (after R.Kippenhahn)

In most important case B mass transfer occurs on thermal time scale:

$$dM/dt \sim M/\tau_{KH},\ \tau_{KH}=GM^2/RL$$

In case A: on nuclear time scale:

$$dM/dt \sim M/t_H$$

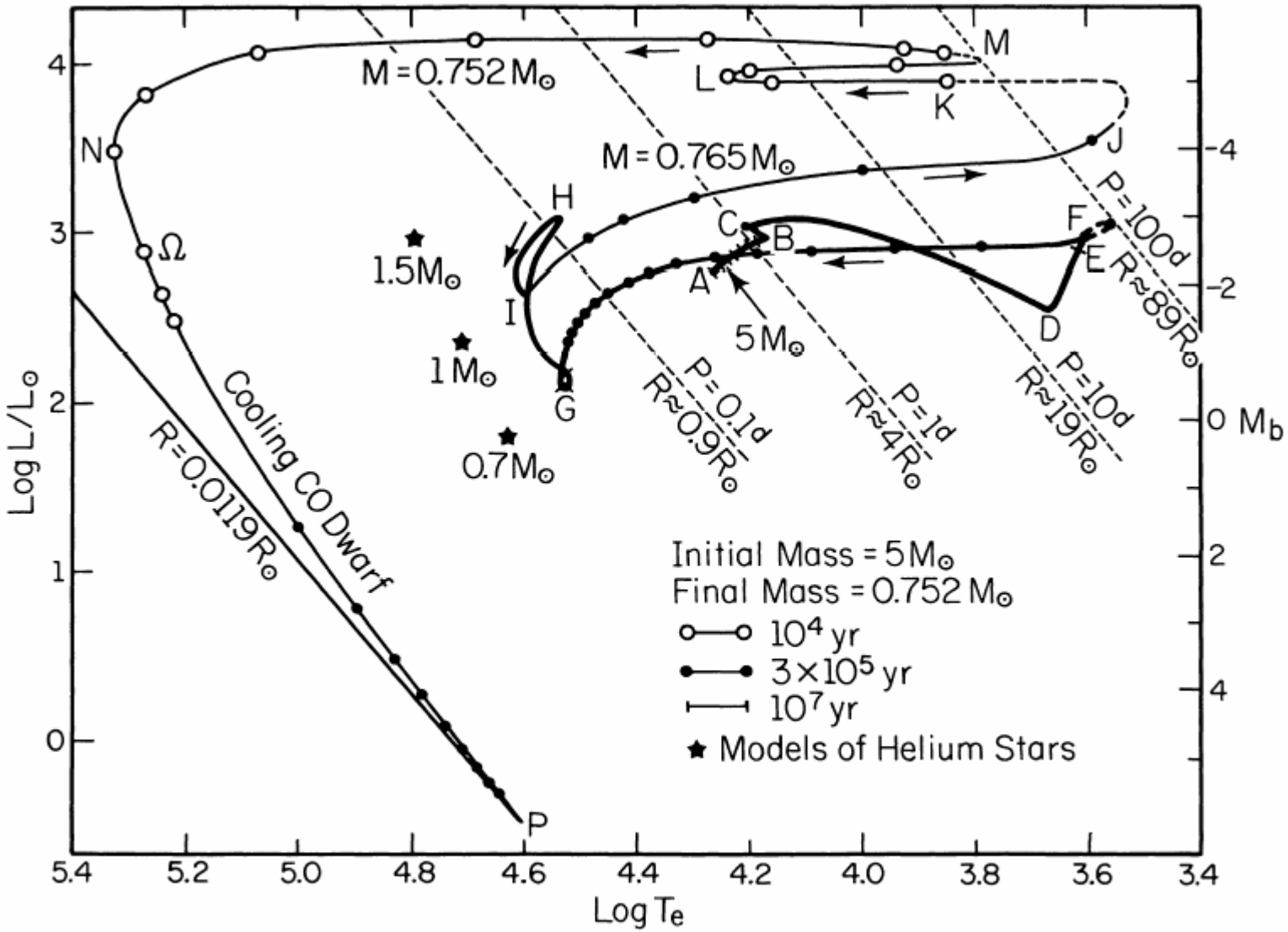

FIG. 1.—Evolution in the H-R diagram of a binary component of initial mass 5 $M_\odot$. Initial composition parameters are $X = 0.7$, $Z = 0.02$. The positions of helium model stars are given by the filled, five-pointed "stars" (Paczyński 1971). Lines of constant orbital period and Roche-lobe radius for a system consisting of two 5 $M_\odot$ unevolved stars are also shown. The temperature of the CO shell reaches a maximum at the point Ω along the track. The main parameters of the stellar model at other labeled points (A, B, ...) are presented in Table 1. Mass loss occurs along dashed portions of the track (E to F; J to K). Time evolution is measured by tick marks (10^7 yr), filled circles (3×10^5 yr), and open circles (10^4 yr).

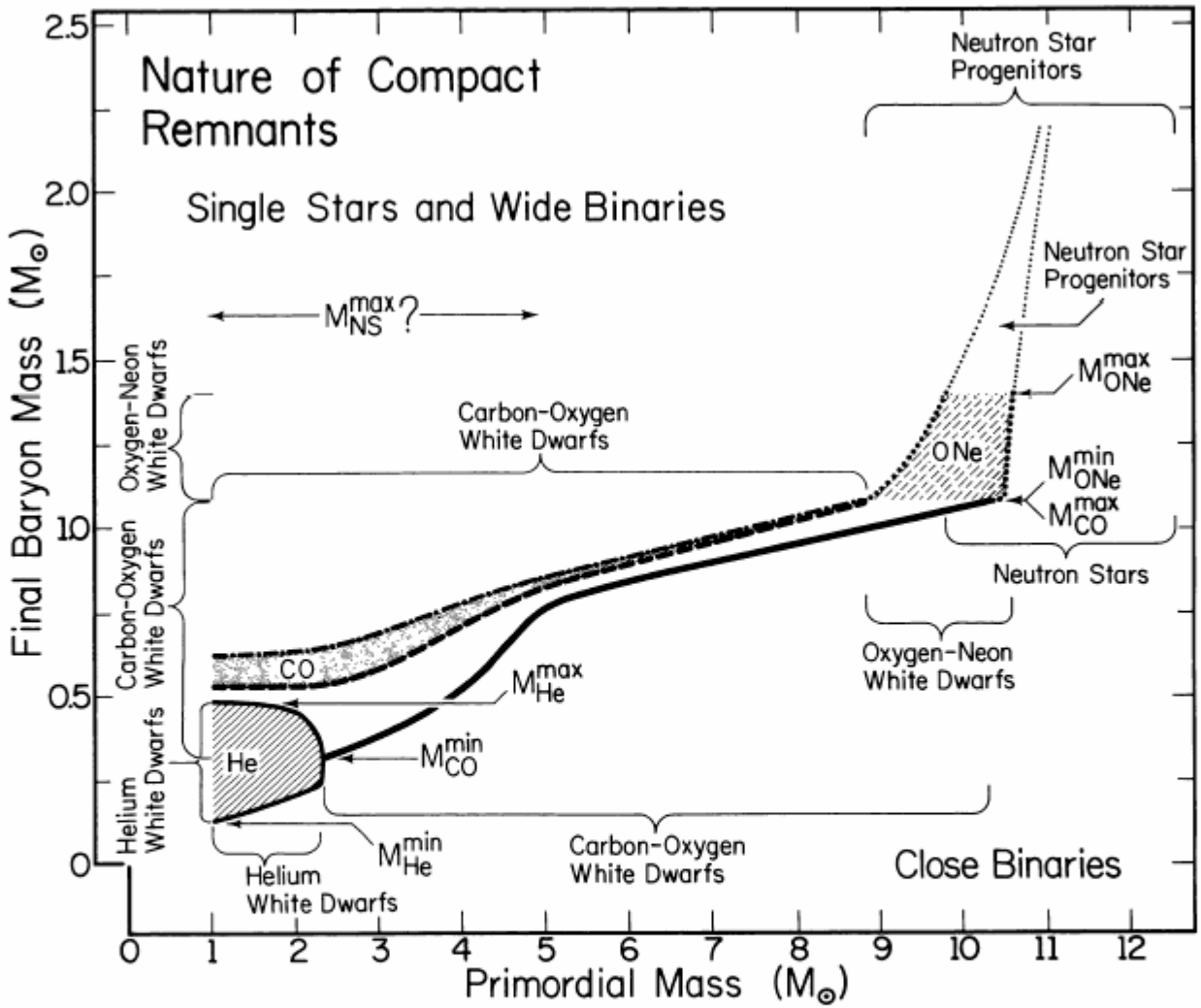

FIG. 30.—The masses and compositions of degenerate dwarfs formed by single stars and by components of interacting binaries. The solid curve extending from 2.3 $M_\odot$ to 10.3 $M_\odot$ is the upper bound on the masses of CO degenerate dwarfs formed in close binaries (first Roche-lobe overflow just before or just after the ignition of central helium). The lower solid curve extending from 1 $M_\odot$ to 2.3 $M_\odot$ is the lower bound on masses of helium degenerate dwarfs formed by stars in close binaries which experience Roche-lobe overflow immediately after forming an electron-degenerate core composed of helium. The upper solid curve extending from 1 $M_\odot$ to 2.3 $M_\odot$ is the upper bound on masses of helium degenerate dwarfs formed in close binaries. The unshaded region gives the possible range in masses of CO degenerate dwarfs formed in wide binaries by components which experience Roche-lobe overflow for the first time during the early AGB phase. The shaded region between the dash and dash-dot curves gives the range in masses of CO degenerate dwarfs formed in wide binaries by components that first experience Roche-lobe overflow during the thermally pulsing AGB (TP–AGB) phase. The dash-dot curve is an estimate of the masses of CO degenerate dwarfs formed by single stars in consequence of mass loss during the TP–AGB phase. Single stars and components of wide binaries cannot form helium degenerate dwarfs or oxygen-neon degenerate dwarfs. In close binaries of appropriate initial configuration, components of initial mass in the range 8.8–10.6 $M_\odot$ may form ONe degenerate dwarfs, with a preponderance being formed by components

Ballistic (planar) trajectories must self-intersect:

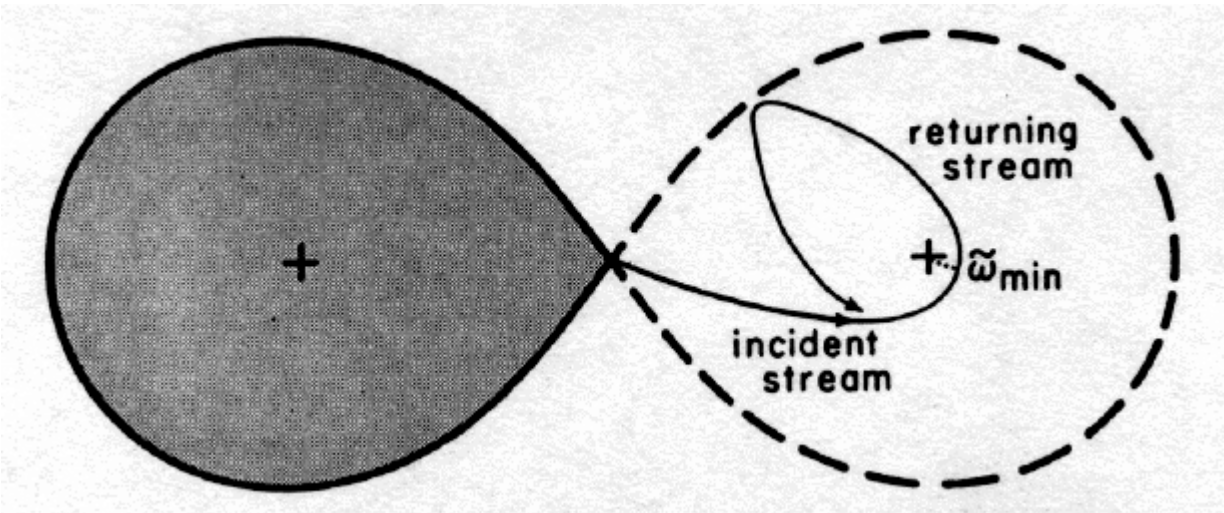

So energy must be lost, but angular momentum is conserved → formation of a ring

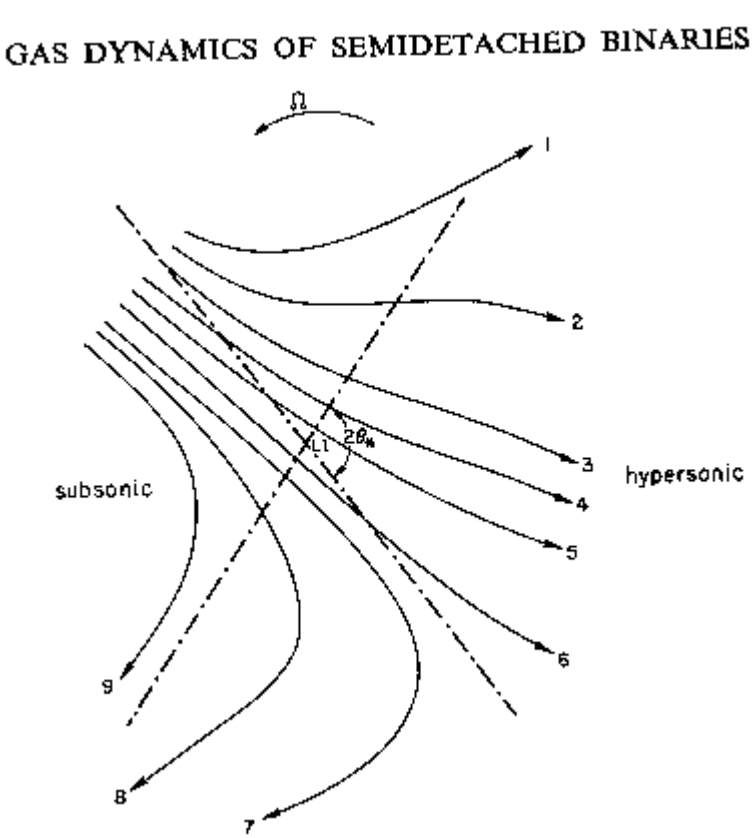
GAS DYNAMICS OF SEMIDETACHED BINARIES
Ω
1
2
3
4
5
6
7
8
9
subsonic
hypersonic
L1
2θ*

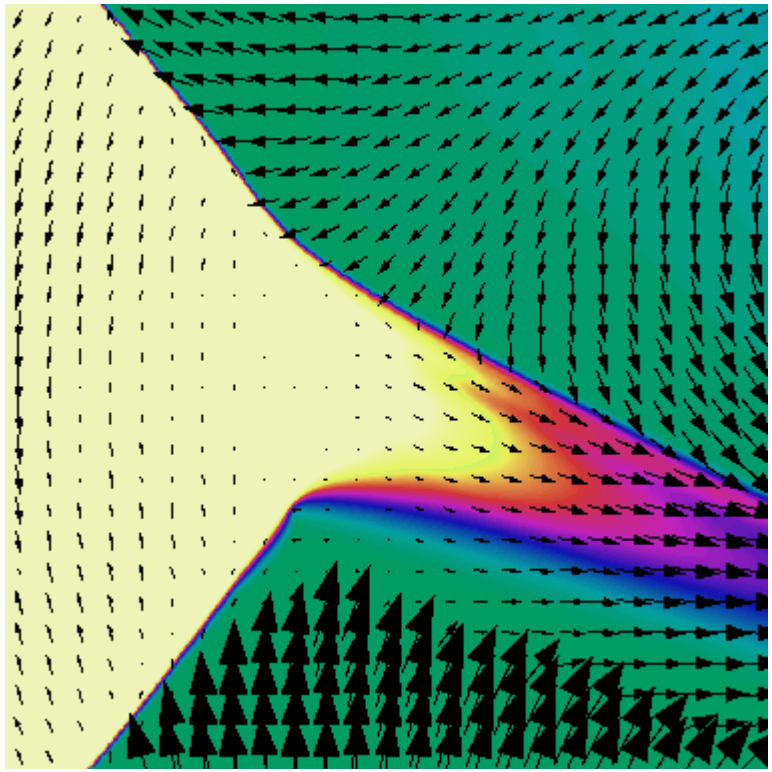

… and 3D SPH hydrodynamics confirms it:

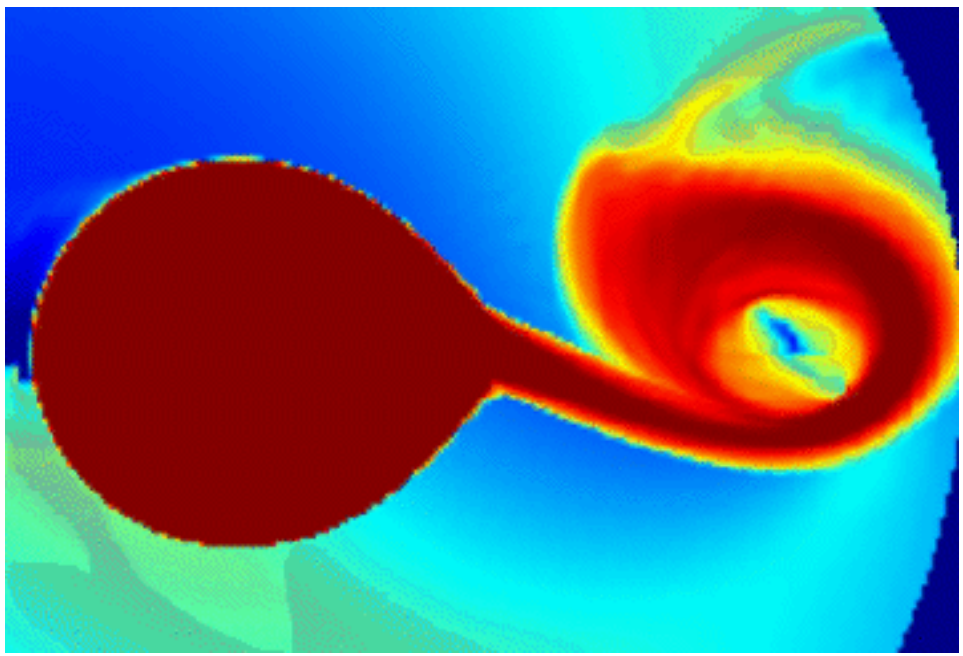

J. Blondin

Formation of accretion disks

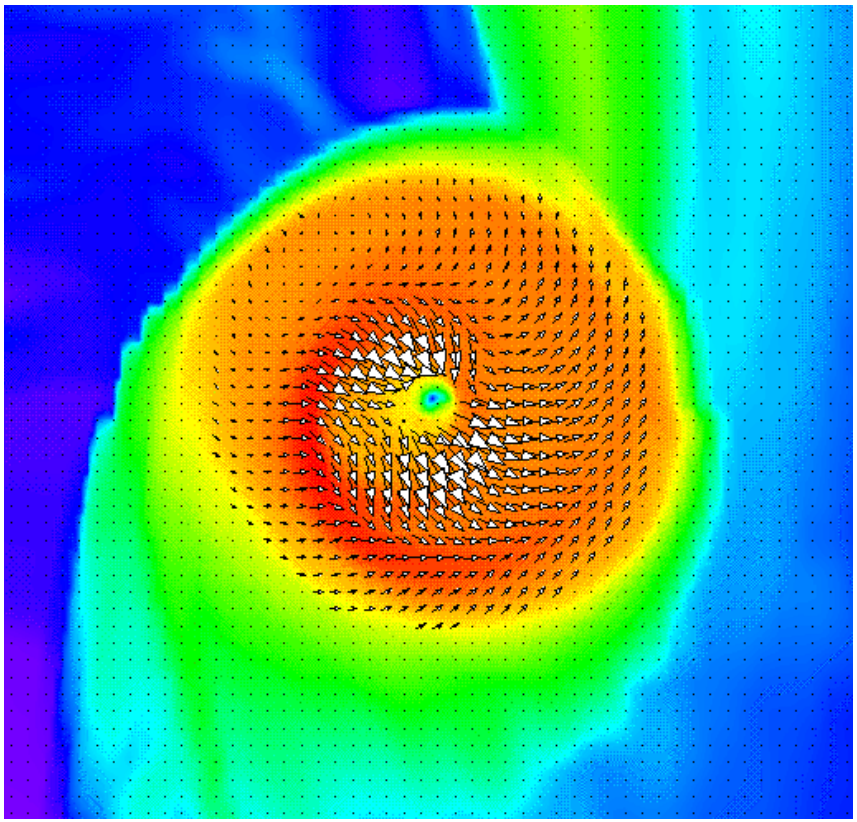

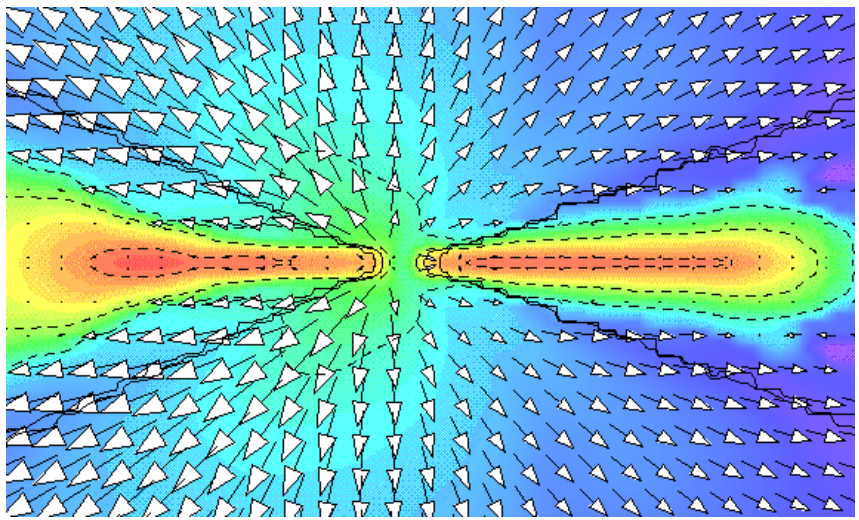

Accretion from stellar wind (without RL overflow) is possible in high mass binaries (e.g. Vela X-1, most X-ray pulsars with Be-stars, Cyg X-1-type BHC, etc)

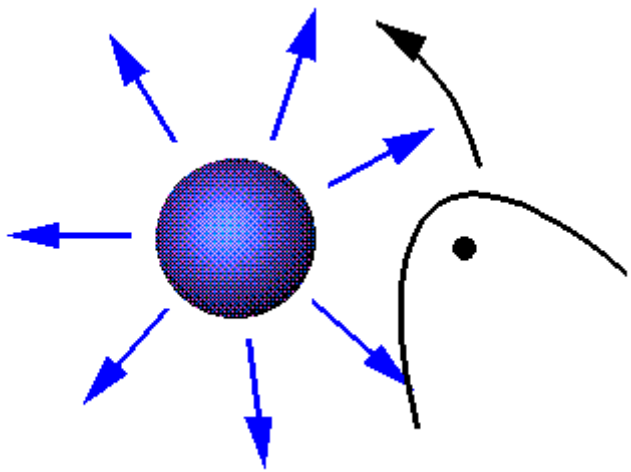

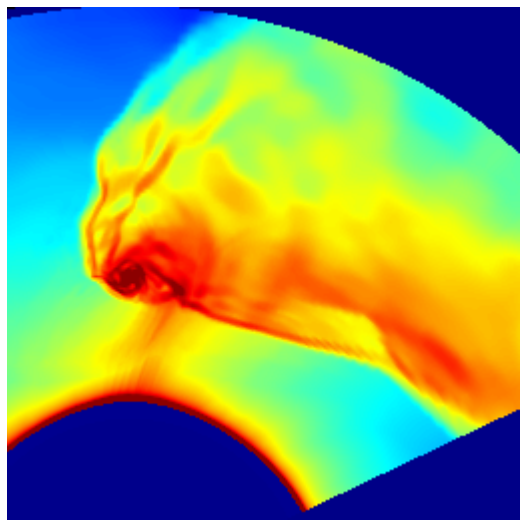

Generally, wind accretion is quasi-stationary

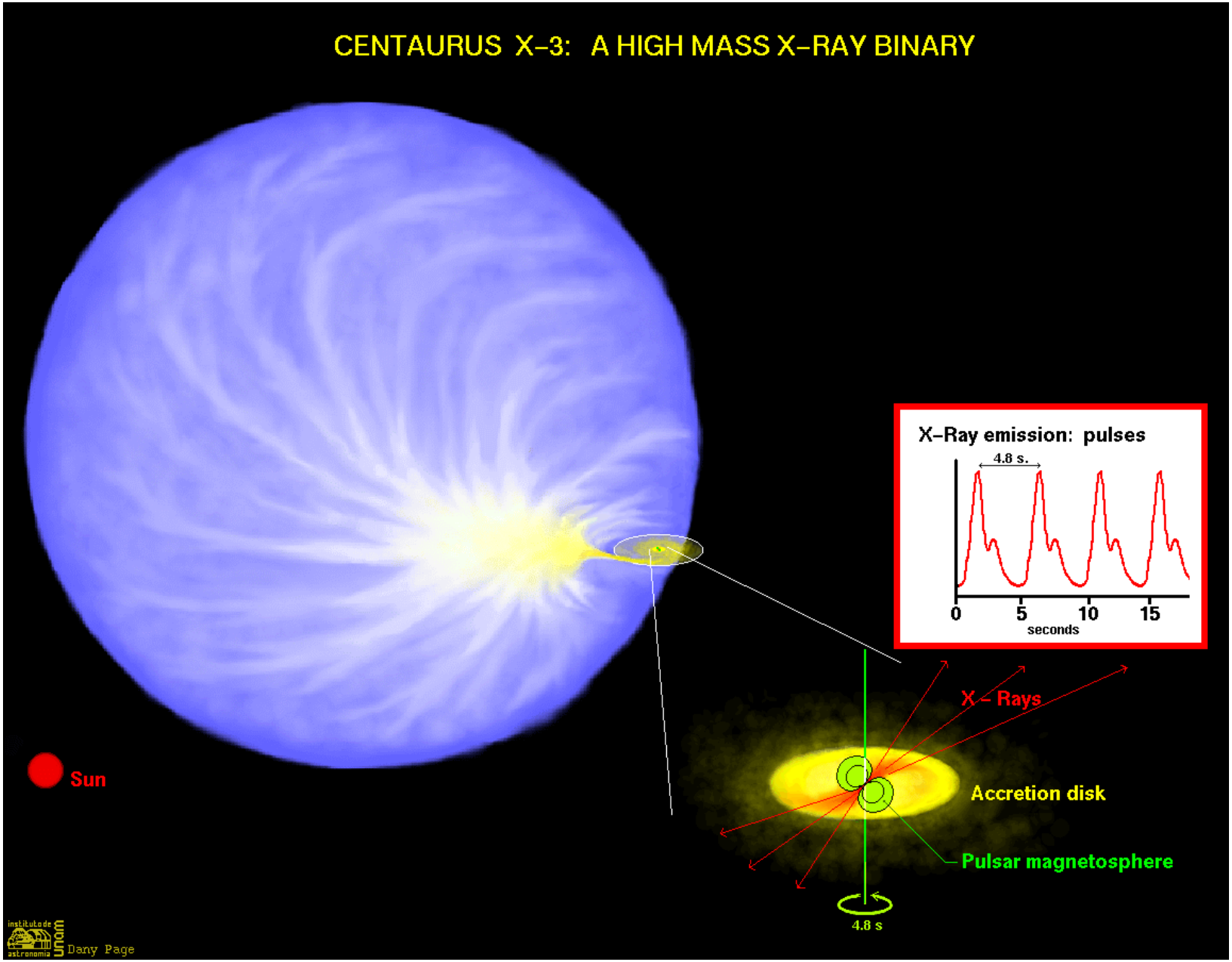
CENTAURUS X-3: A HIGH MASS X-RAY BINARY
X-Ray emission: pulses
4.8 s.
0
5
10
15
seconds
X - Rays
Sun
Accretion disk
Pulsar magnetosphere
4.8 s
Dany Page

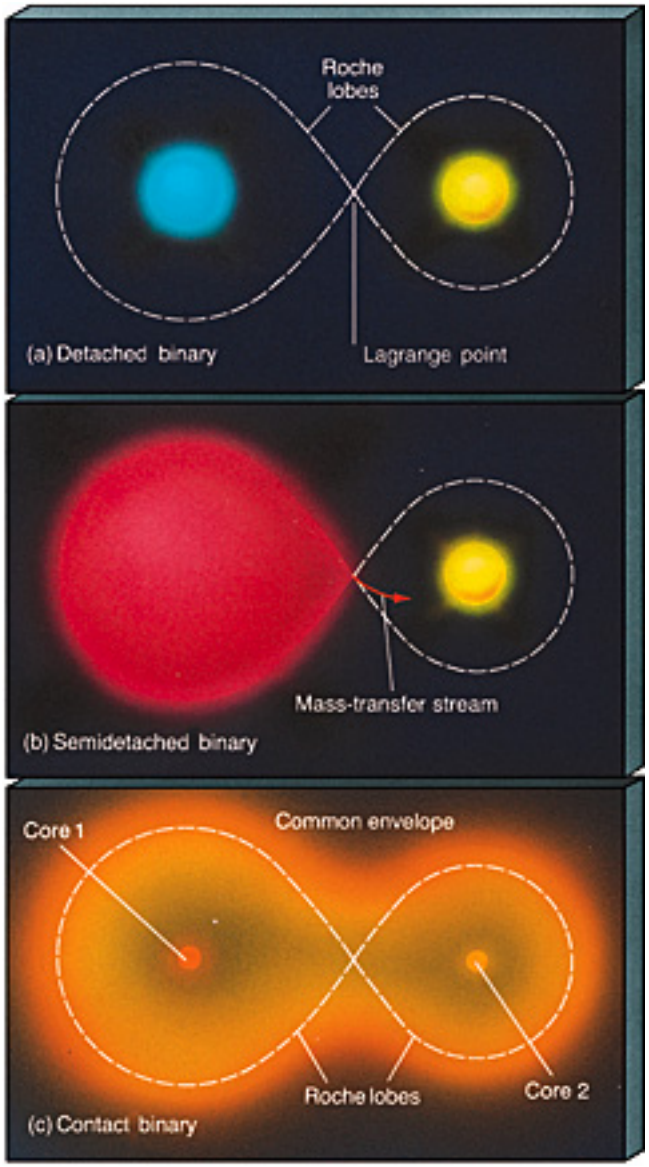

Problem: How to make close binaries with compact stars (CVs, XRBs)? Most angular momentum from the system should be lost.

Non-conservative evolution: Common envelope stage

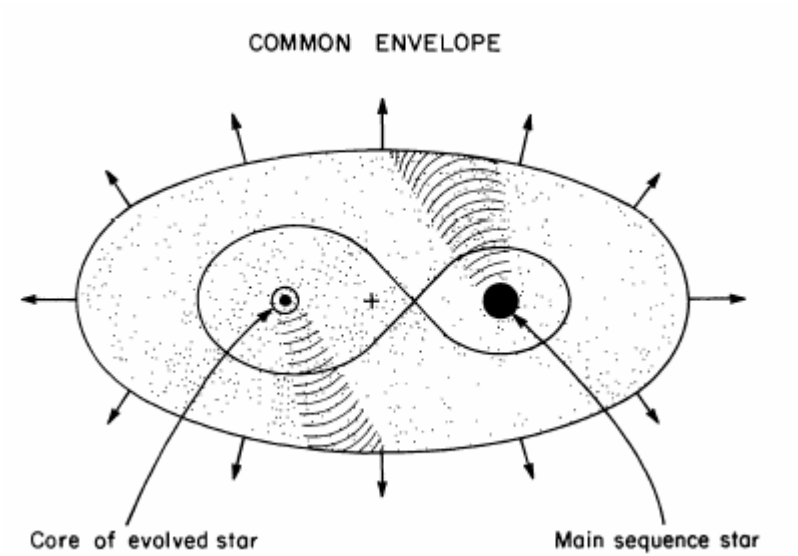

Common treatment: orbital energy release during the orbital shrinkage is spent to expell the envelope

$$\overbrace{\text{efficiency}}^{\alpha_{\rm CE}} \times (\text{orbital energy release during CE}) =$$

$$-\frac{1}{2}\frac{GM_1M_2}{a_{initial}} - \left(-\frac{1}{2}\frac{GM_1M_2^f}{a_{final}}\right)$$

$$= \text{binding energy of the envelope}$$

$$-\frac{GM_2(M_2 - M_2^f)}{\lambda R_2}$$

Numerical (multi D) hydro simulation give $\alpha_{\rm CE} \sim 0.3 - 0.5$

However, it is not clear whether CE efficiency is constant and whether the simplest energy conservation suffices to treat CE correctly.

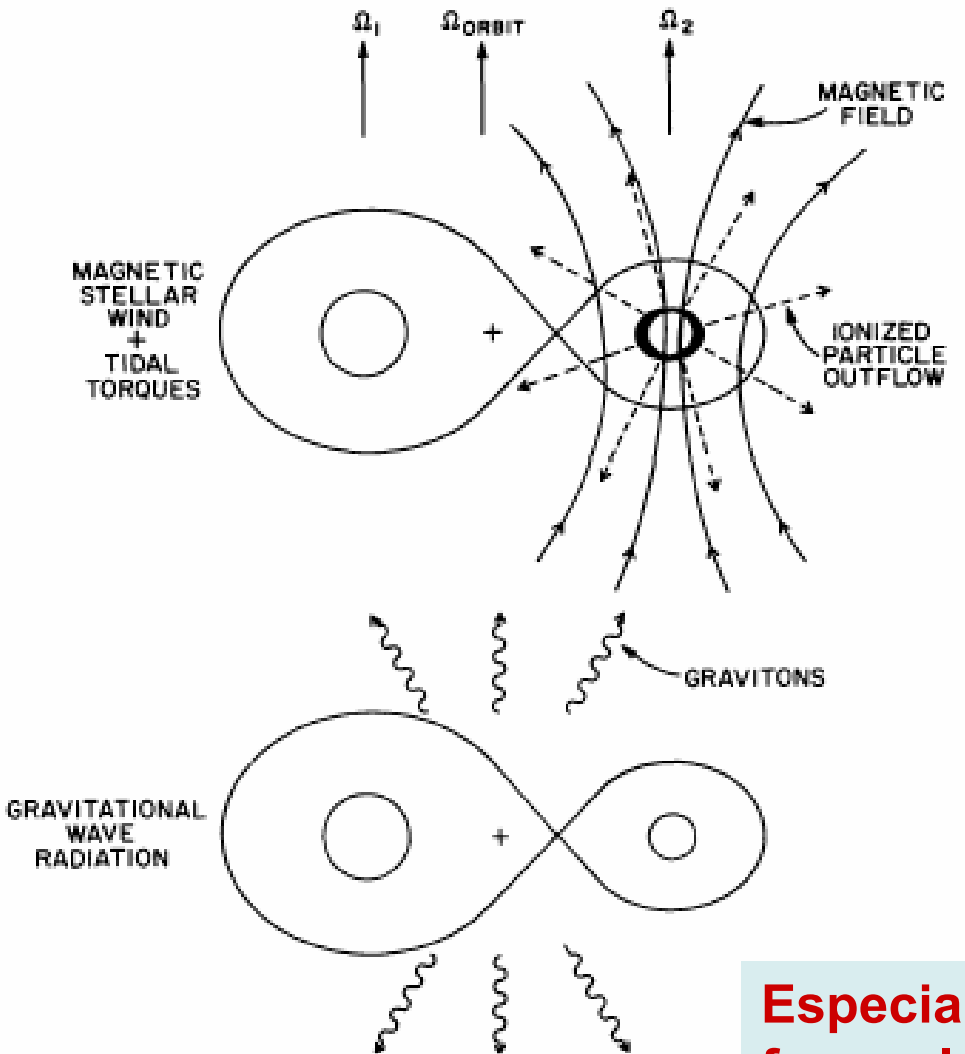

Angular momentum loss:

- Magnetic stellar wind (effective for main sequence stars with convective envelopes $0.3<M<1.5\ M_\odot$)

- Gravitational radiation (drives evolution of binaries with P<15 hrs)

Especially important for evolution of low-mass close binaries!

Intermezzo: Gravitational radiation from a binary star.

An easy way to get a complex formula.

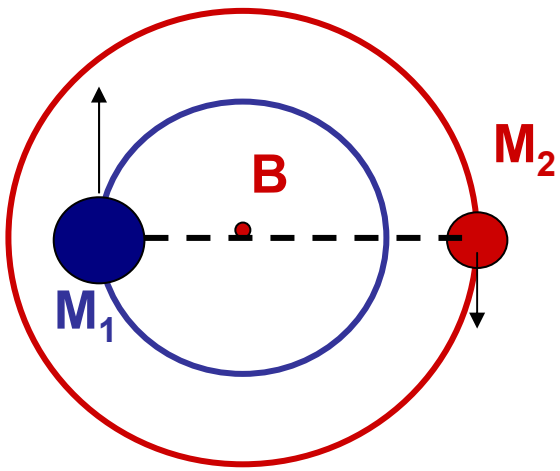

Binary star: $M_1, M_2, a.$ Assume circular orbit.

$M_1 a_1 = M_2 a_2, \quad a = a_1 + a_2 = const$ in Newtonian case.

Kepler's 3d law: $\omega^2 \equiv \left(\frac{2\pi}{T}\right)^2 = \frac{G(M_1 + M_2)}{a^3}$

Gravitational radiation is due to variable quadrupole moment of the system. Q.m. is the same twice the orbital period $\Rightarrow$

$$\omega_{GW} = 2\omega, \quad \lambda_{GW} = \frac{2\pi c}{2\omega} = \frac{cT}{2}$$

Wave zone: $r > R_l \sim \frac{c}{\omega}$ Field ~ 1/r for radiation

Inside W.z. ($r<R_1$) the field is just variable tidal accelerations:

mass 1: $\sim \frac{GM_1}{r^3}$ $a_1 \sim \frac{G\mu}{r^3} a$

mass 2: $\sim \frac{GM_2}{r^3}$ $a_2 \sim \frac{G\mu}{r^3} a,$

where $\mu \equiv \frac{M_1 M_2}{M}$ is reduced mass, $M \equiv M_1 + M_2$ is the total mass

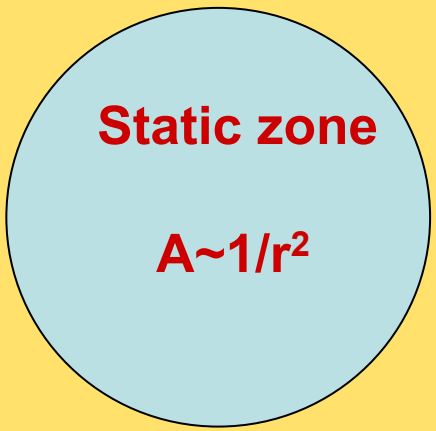

Radiation of **any field** outside the wave zone:

Field: $A \sim 1/r$

Energy flux: $S \sim A^2$

Energy loss: $dE/dt \sim r^2 S$

GW from a binary: $A_{GW} \sim A_1 - A_2$,

$$A_1 \sim \frac{G}{c^2}\frac{\mu\omega^2 a}{r}e^{i2\omega t} \sim \frac{\mu\omega^2 a}{r}e^{i2\omega t}$$ (to sew at $R=R_1$!)

$$A_2 \sim \frac{\mu\omega^2 a}{r}e^{i(2\omega t-\Delta\phi)}, \quad \text{phase delay } \Delta\phi \sim (a_1+a_2)\omega \sim \frac{a}{\lambda_{GW}}$$

In the w.z. $r \gg \lambda_{GW} \gg a$

$$A_{GW} \sim \frac{\mu\omega^2 a}{r}\Delta\phi \sim \frac{\mu\omega^3 a^2}{r}$$

$$\left\langle \frac{dE}{dt} \right\rangle_{GW} \sim A_{GW}^2 r^2 \sim \mu^2\omega^6 a^4 \sim \frac{\mu^2 M^3}{a^5} = -\frac{G^4}{c^5}\frac{\mu^2 M^3}{a^5}$$

Exact expression reads:

$$\left\langle \frac{dE}{dt} \right\rangle_{GW} = -\frac{32G^4}{5c^5}\frac{\mu^2 M^3}{a^5}$$

Angular momentum loss rate:

$$\left\langle \frac{dL}{dt} \right\rangle_{\rm GW} = \frac{1}{\omega}\left\langle \frac{dE}{dt} \right\rangle_{\rm GW} = -\frac{32G^{7/2}}{5c^5}\frac{\mu^2 M^{5/2}}{a^{7/2}}$$

Binary orbital angular momentum decreases:

$$\left(\frac{d\ln L_{orb}}{dt}\right)_{\rm GW} = \frac{\left\langle \frac{dL}{dt} \right\rangle_{\rm GW}}{L_{orb}} = -\frac{32G^4}{5c^5}\frac{\mu M^2}{a^4}$$

Characteristic GW timescale:

$$\tau_{\rm GW} = \left(\frac{d\ln L_{orb}}{dt}\right)^{-1}_{\rm GW} \approx \mathbf{1.2\times 10^9\ yrs}\left(\frac{\mathbf{M_1}}{\mathbf{M_\odot}}\right)^{-1}\left(\frac{\mathbf{M_2}}{\mathbf{M_\odot}}\right)^{-1}\left(\frac{\mathbf{M}}{\mathbf{M_\odot}}\right)^{-1}\left(\frac{\mathbf{a}}{\mathbf{R_\odot}}\right)^{4}$$

τ

Magnetic stellar wind

Axial rotation braking of single G-dwarfs (Skumanich, 1972)

$$V \sim t^{-1/2}, \quad \text{where } t \text{ is the age}$$

Physics: stellar wind plasma ``streams" along magnetic field lines until $\rho v^2 \sim B^2(r)/4\pi$, so carries away much larger specific angular momentum (Mestel).

Assume the secondary star in a low-mass binary $(0.4 \le M_2 \le 1.5 M_\odot)$ experiences m.s.w. Tidal forces tend to keep the star in corotation with orbital revolution: $\omega_2 = \omega$. Angular momentum conservation then leads to:

$$\frac{dL_{orb}}{dt} = \frac{dJ_2}{dt}$$

Recolling that: $L_{orb} = \mu \omega a^2$ and using Kepler's 3d law we get

$$\frac{d\ln L_{orb}}{dt} \sim -\frac{R_2^4}{M_1}\frac{GM^2}{a^5} \quad \Rightarrow \quad \tau_{MSW} = \left(\frac{d \ln L_{orb}}{dt}\right)^{-1} \approx 1.5 \times 10^6 \text{ yrs} \left(\frac{M_1}{M_\odot}\right)\left(\frac{M}{M_\odot}\right)^{-2}\left(\frac{a}{R_\odot}\right)^{5}\left(\frac{R_2}{R_\odot}\right)^{-4}$$

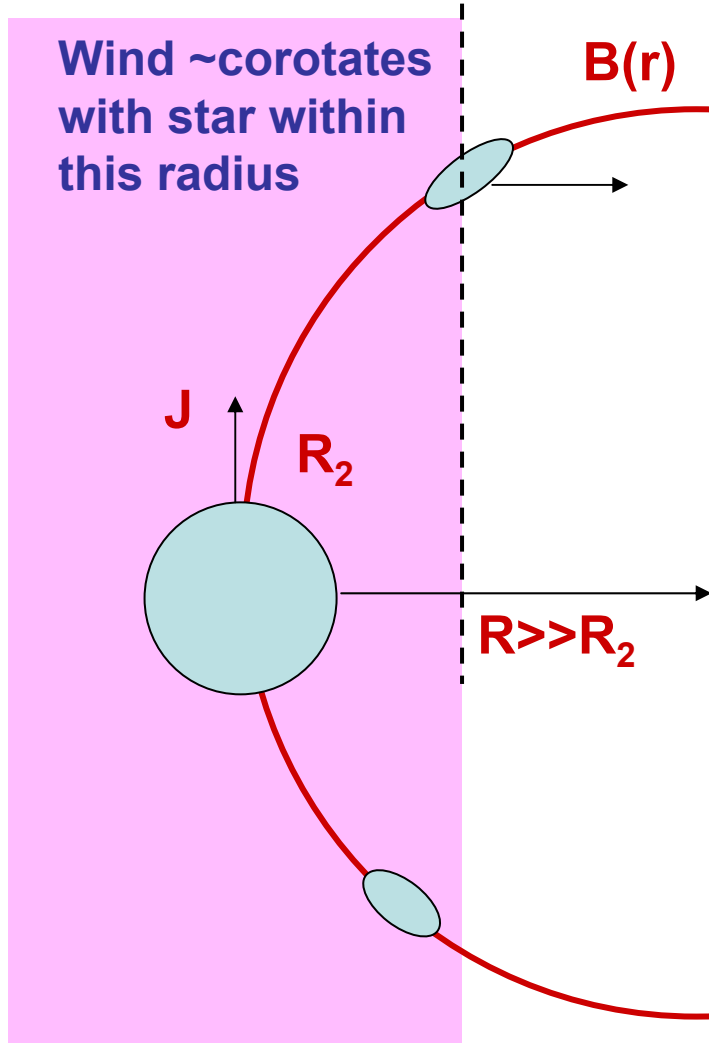

Mass loss due to MSW and GW

Mass transfer due to orbital angular momentum losses occurs because Roche lobe radius is proportional to binary separation: $\mathrm{R_L} = af(M_1, M_2)$. So by requiring

$$\mathrm{R}(\mathrm{M}_2) = R_L(M_2) \text{ and}$$

$$\frac{\partial R(M_2)}{\partial \ln M_2} = \frac{\partial R_L(M_2)}{\partial \ln M_2} \text{ (for stability)}$$

one usually derives mass transfer rate: $\dot{\mathrm{M}}(\mathrm{M}_1, M_2, a)$ for specified angular momentum loss mechanism.

Roughly, $\dot{\mathrm{M}} \sim \frac{\mathrm{M}_2}{\tau}$, where τ is the characteristic timescale, so

$$\dot{M}_{GW} \sim 10^{-9} M_\odot / \mathrm{yr} \left(\frac{M_1}{M_\odot}\right)\left(\frac{M_2}{M_\odot}\right)^2\left(\frac{M}{M_\odot}\right)\left(\frac{a}{R_\odot}\right)^{-4} \propto a^{-4}$$

$$\dot{M}_{MSW} \sim 6\times10^{-7} M_\odot / \mathrm{yr} \left(\frac{M_1}{M_\odot}\right)\left(\frac{M}{M_\odot}\right)^2\left(\frac{R_2}{R_\odot}\right)^4\left(\frac{a}{R_\odot}\right)^{-5} \propto a^{-1}$$

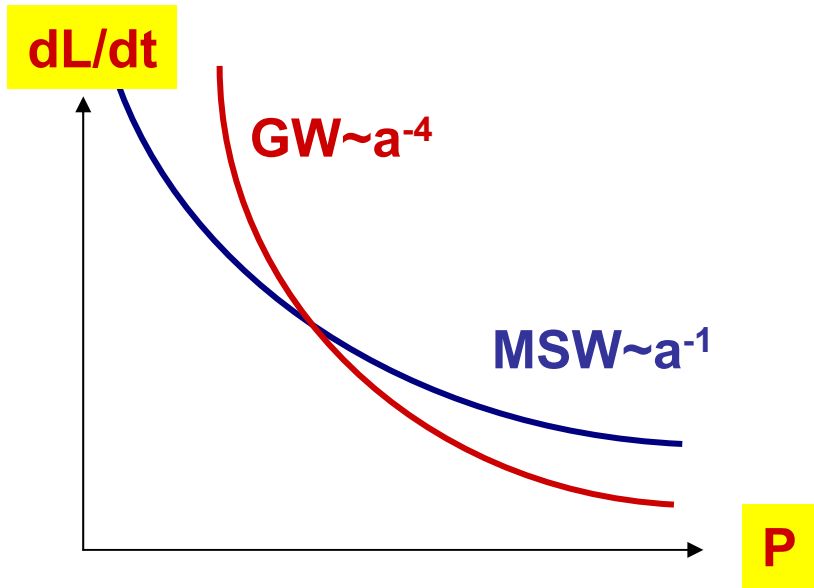

MSW is more effective at larger orbital periods, but GW always wins at shorter periods! Moreover, MSW stops when M_2 ~0.3-0.4 $M_\odot$ where star becomes fully convective and dynamo switches off.

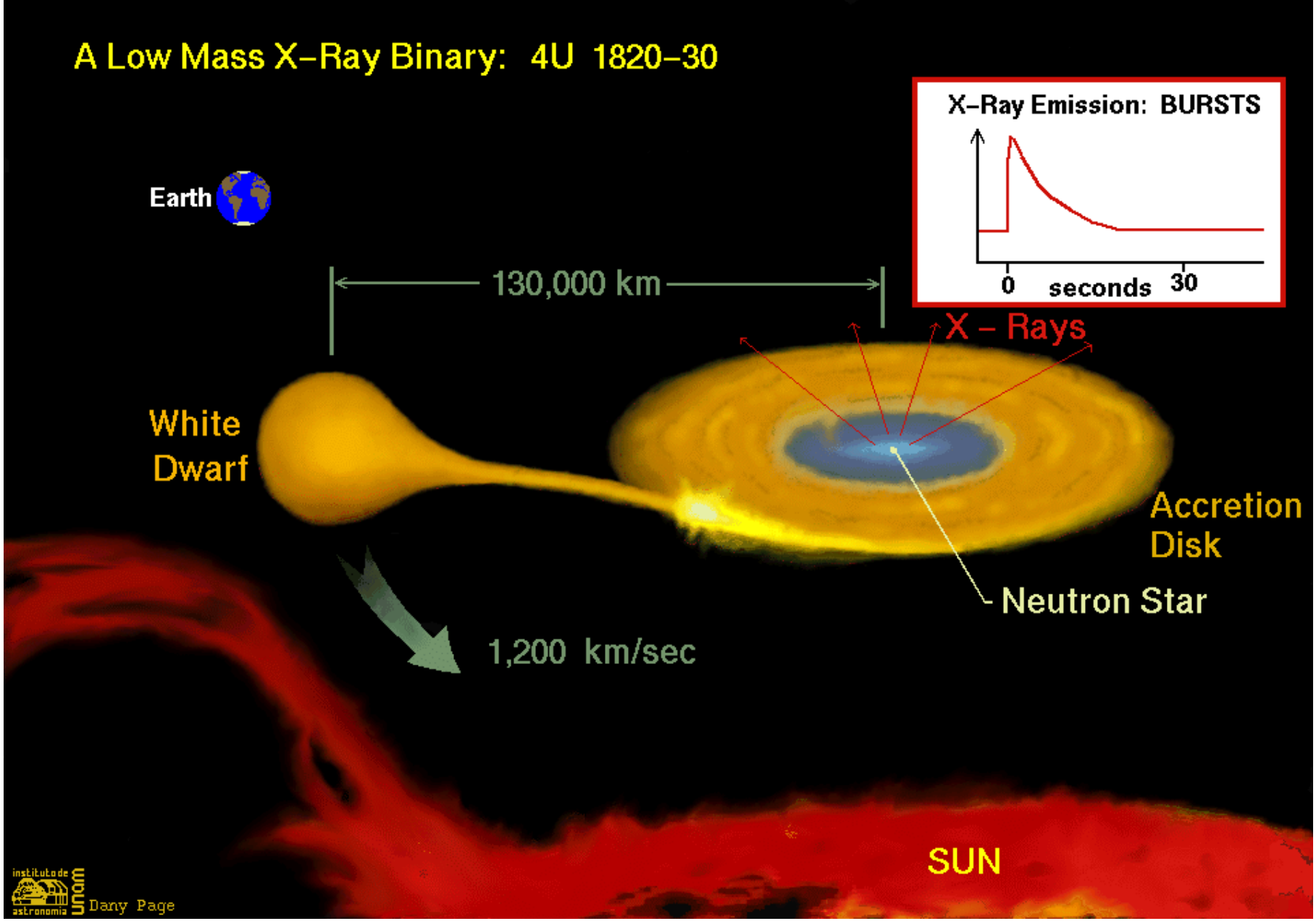
A Low Mass X-Ray Binary: 4U 1820-30
X-Ray Emission: BURSTS
0
seconds
30
Earth
130,000 km
X - Rays
White
Dwarf
Accretion
Disk
Neutron Star
1,200 km/sec
SUN
Dany Page

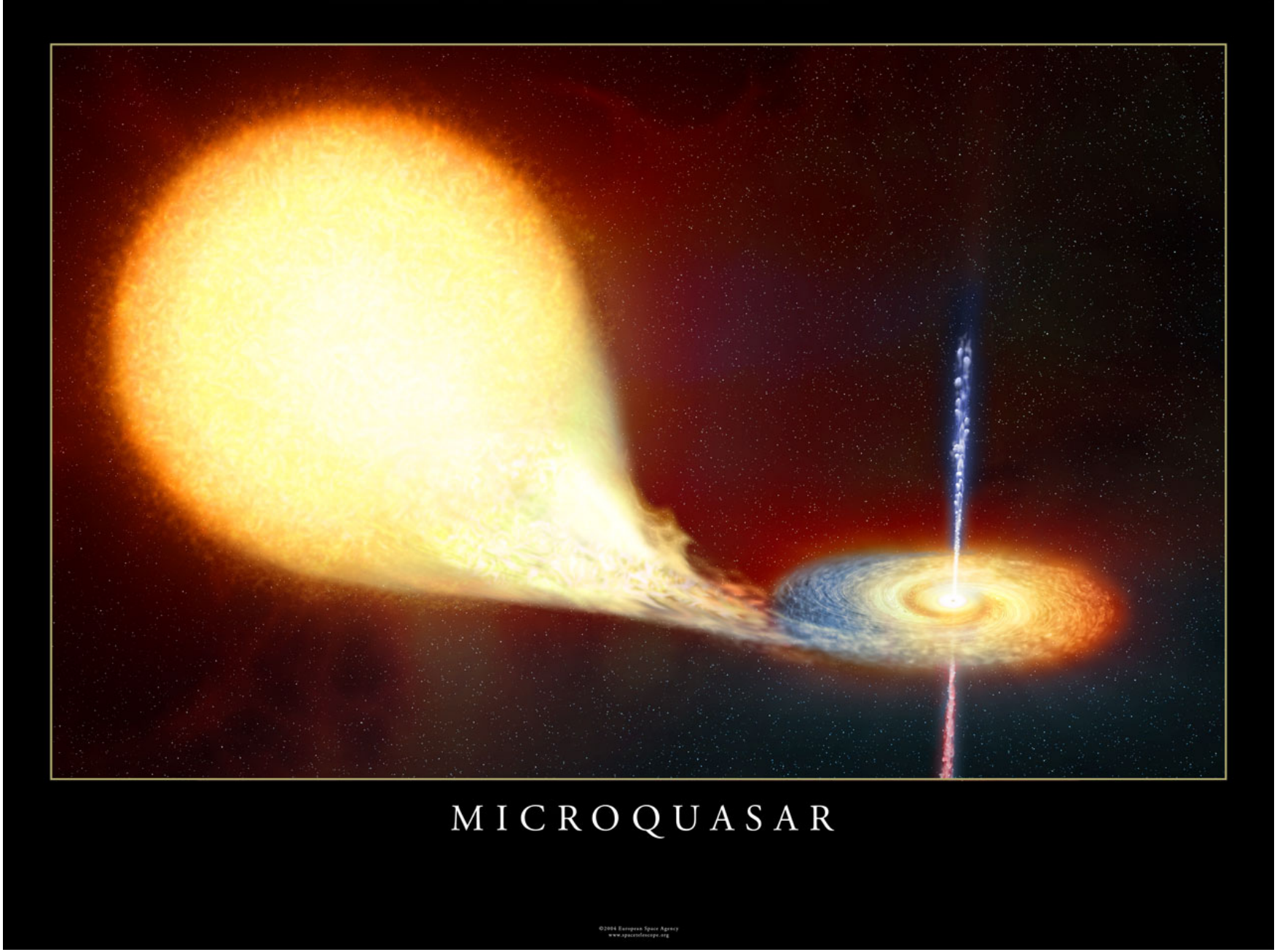
MICROQUASAR

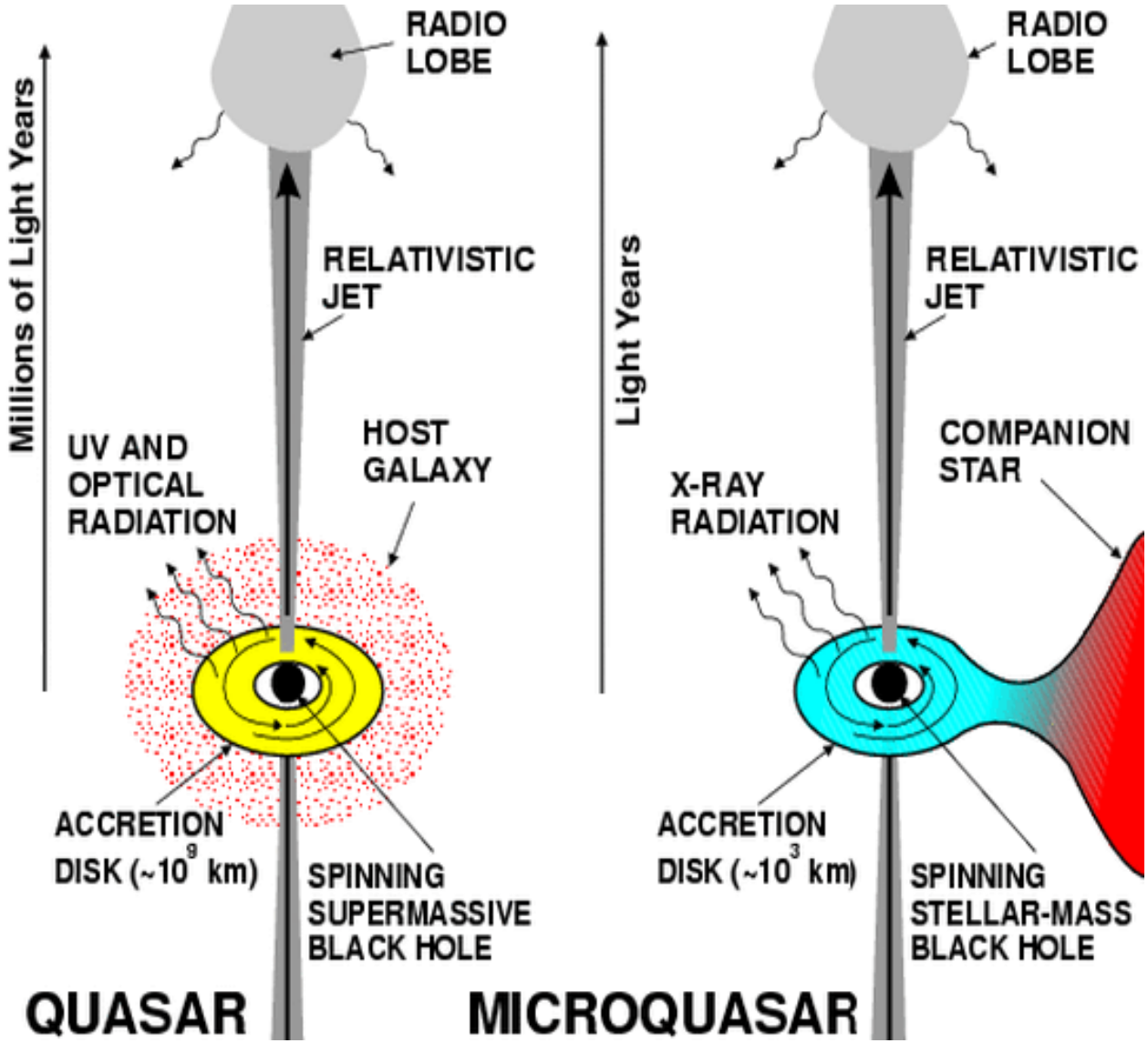
RADIO LOBE
RELATIVISTIC JET
Millions of Light Years
UV AND OPTICAL RADIATION
HOST GALAXY
ACCRETION DISK (~10^9 km)
SPINNING SUPERMASSIVE BLACK HOLE
QUASAR
RADIO LOBE
RELATIVISTIC JET
Light Years
X-RAY RADIATION
COMPANION STAR
ACCRETION DISK (~10^3 km)
SPINNING STELLAR-MASS BLACK HOLE
MICROQUASAR

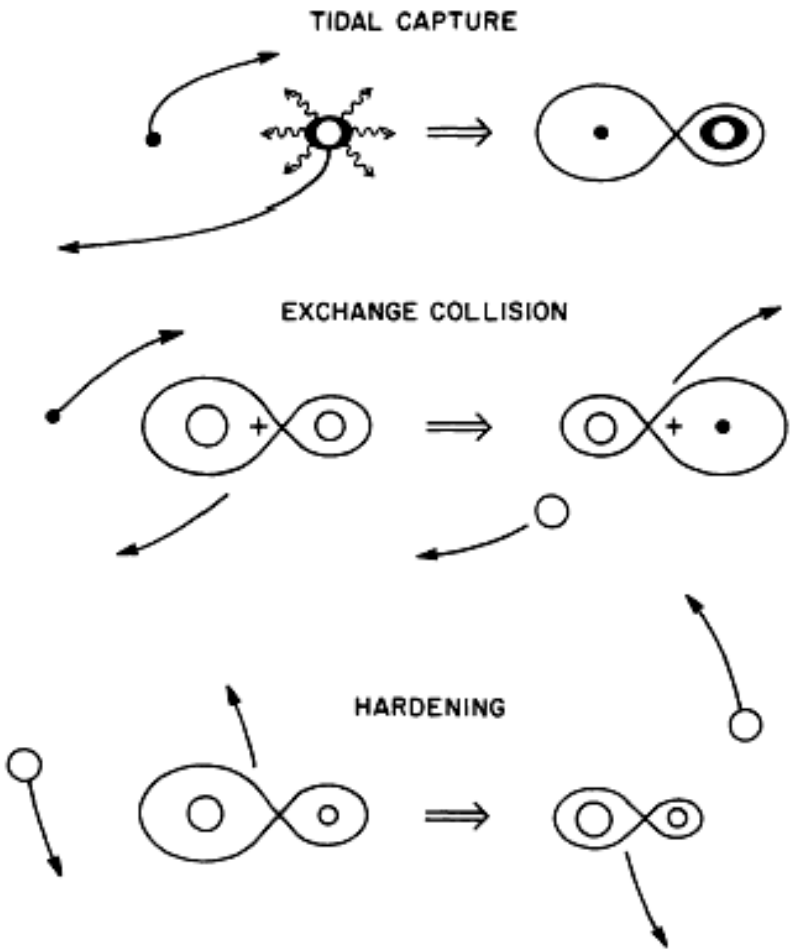

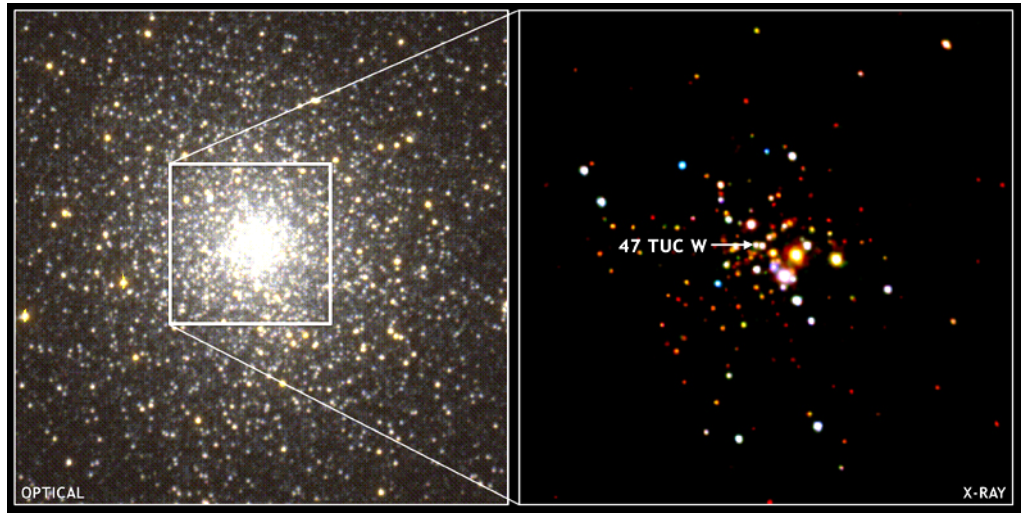

Hundreds close XRB and millisecod pulsars are found in globular clusters

Formation of close low-mass binaries is favored in dense stellar systems due to various dynamical processes

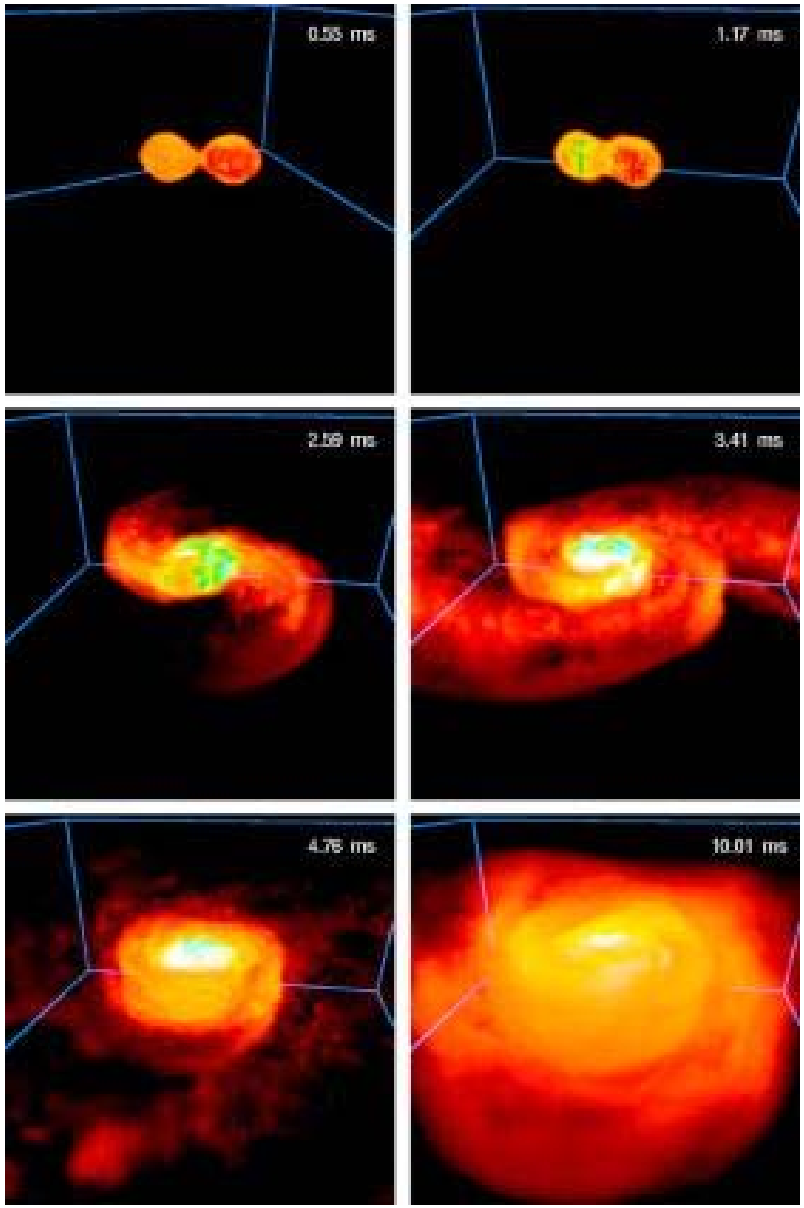

Binary pulsars

PSR 1913+16 (1974)

2005: 7 binary NS systems

R.A. Hulse J.B. Taylor

Nobel prize in physics 1993

Evolution of binary parameters in double NS is fully controlled by GW emission.

Coalescent binary neutron stars and black holes are thought to be the primary astrophysical sources of gravitational waves

Binary evolution: Major uncertainties

- All uncertainties in stellar evolution (convection treatment, rotation, magnetic fields…)
- Limitations of the Roche approximation (synchronous rotation, central density concentration, orbital circularity)
- Non-conservative evolution (stellar winds, common envelope treatment, magnetic braking…)
- For binaries with NS (and probably BH): effects of supernova asymmetry (natal kicks of compact objects), rotational evolution of magnetized compact stars (WD, NS)